

# Analysis of Loudspeaker Line Arrays

Mark S. Ureda

*JBL Professional, Northridge, CA USA*

This paper provides a set of mathematical expressions to analyze the performance of loudspeaker line arrays. It begins by developing a set of expressions for straight-line arrays including the directivity function, polar response, quarter-power angle, on-axis and off-axis pressure response and two-dimensional pressure field. Since in practice many loudspeaker line arrays are not actually straight, the paper then provides expressions for curved (arc), “J” and “progressive” line arrays. In addition, since loudspeaker systems are often not perfect sources, the paper analyzes the effects of spherical radiating sources and gaps between sources. The paper closes with several examples of how to apply the models and compares modeled performance to measured polar data.

## 1 INTRODUCTION

Vertical line arrays of loudspeakers are gaining prominence these days among sound reinforcement professionals. That is not to say that they are an entirely new concept. Indeed, David Klepper and Douglas Steele wrote in 1963 [1]: “Line-source loudspeaker arrays, often called ‘column’ loudspeakers, have recently become of great interest to sound-system contractors and equipment manufacturers in this country.”

What *is* new is that loudspeaker manufacturers have applied good engineering practice to long-known principles of line source physics. Systems today provide well-behaved directivity response, high output power and high quality sound over an extended frequency range. Together these represent a significant improvement in performance over conventional column speakers.

Column speakers typically comprise a vertical stack of full-range direct radiators. They produce modest sound power levels and exhibit vertical directivity response that changes substantially with frequency. Klepper and Steele describe problems with column speakers including “narrowing of the major (on-axis) lobe at higher frequencies” and “strong minor off-axis lobes or side lobes at high frequencies.” These, they write, are predicted by equations given by Olson [2]. Their paper prescribes methods for improving the polar response, but the success of these techniques is limited by the directional characteristics of the individual loudspeakers themselves that narrow at high frequency.

Today, manufacturers of loudspeaker line arrays often provide specially designed wave-guides in place of individual direct radiators for the high frequency band. This is an important improvement. While column loudspeakers behave like an array of individual, frequency-dependent acoustic sources, contemporary systems behave more like continuous line sources. This

allows them to achieve well-behaved directivity response to very high frequency.

Manufacturers have also realized that long, perfectly straight loudspeaker line arrays produce a directivity response that often becomes too narrow at high frequency for many sound reinforcement venues. In fact, they have learned that it is often desirable to produce an asymmetrical response in the vertical plane, for instance, one that projects energy forward and downward at the same time. This can be achieved if the array is slightly curved, particularly along the lower portion. Recently, manufacturers have designed line array loudspeaker systems that can be curved over the entire length of the array while maintaining the attributes of a continuous source. This allows users to achieve simultaneously the narrow, long throw characteristics of a straight-line array and the wide, lower fill characteristics of a curved array.

This paper provides mathematical expressions for estimating the performance of a wide variety of line arrays. The models are based on theoretical line sources but the estimates obtained agree quite well with measurements taken on real-life line arrays, particularly those from the latest generation of loudspeaker systems designed specifically for line array applications.

## 2 BACKGROUND AND OVERVIEW

Most analyses of line sources reference Wolff and Malter’s [3] seminal work of 1929. Wolff et. al. develop expressions for the polar response of a linear array of point sources in the far field. The far field restriction allows the directivity function to be expressed in closed form. Their paper has been referenced and/or augmented over the years by Beranek [4], Wood [5], Davis [6], Rossi [7], and Skudrzyk [8] among others. For the convenience of the reader, Sections 3.1 through 3.4 of this paper summarize important elements of their work as well.

Section 3.5 analyzes the on-axis pressure response of line sources. Here, the far field restriction is abandoned and the pressure is expressed as a function of distance. This analysis follows the work of Lipshitz and Vanderkooy [9], and Smith [10] who present the on-axis and off-axis pressure response of line sources. They show that the pressure response undulates near the source while generally decreasing in level at -3dB per doubling of distance. At a certain distance, referred to as the transition distance<sup>(1)</sup>, the undulations disappear and the response falls off at -6dB. The *near field* is defined as the region between the source and the transition distance. Beyond the transition distance is the *far field*. The transition distance is a function of line source length and frequency and has been estimated by Smith [10], Heil [11], Junger [12], and Ureda [13].

The pressure response of a line source on either side of the transition distance, however, is more complex than the on-axis pressure response would suggest. In fact, depending upon the point chosen along the source from which one begins the pressure response analysis, different results are obtained. Section 3.5 explores this complexity by comparing the results obtained when different points along a straight-line source are taken as the initial point. It is shown that each of these responses represent different slices through the pressure field. The mathematical expression for the pressure field of a straight-line source is given in Section 3.6.

As illustrated throughout Section 3, straight-line sources produce polar response curves that vary substantially with length and frequency. At long lengths and high frequency they get very narrow, often too narrow for sound reinforcement venues. Curved or arc sources, however, produce polar response curves that are materially wider and approach the included angle of the arc at high frequency. This has been described in many of the texts cited earlier including Wolff [14], Olson [15], and Rossi [16]. Section 4 of this paper expands on the analysis of arc sources by providing mathematical expressions for the polar response, on-axis pressure response and two-dimensional pressure field.

Arc sources, while useful by themselves in certain sound reinforcement venues, are of particular interest when used in conjunction with straight-line sources. The combination is referred to as a J-source [17]. J-sources are comprised of a straight-line source placed above and adjacent to an arc source. The straight segment provides long throw and the arc segment provides coverage in the down-front region. Together they provide an asymmetrical polar response in the vertical plane that is well suited for many venues. Section 5 describes J-sources and provides expressions for the polar response, on-axis response and two-dimensional pressure field.

Like a J-source, a progressive<sup>(2)</sup> source [18] also provides an asymmetrical polar response in the vertical plane. Unlike a J-source, however, a progressive source is a continuous curve. The upper portion of the source is nearly straight but then increases in curvature toward the bottom. Section 6 provides expressions for its polar response, on-axis pressure response and two-dimensional pressure field. These show that a progressive source produces a response that is remarkably constant with frequency.

In practice, even with specially designed loudspeaker systems, large line arrays are not perfectly continuous line sources. They invariably have gaps between the individual array elements that are essentially non-radiating portions of the total line source. Certain effects of such discontinuities are described by Urban, [19]. Section 7 of the present paper expands on this work and analyzes the polar response of straight-line sources with various size gaps. It provides guidelines for acceptable gap-to-wavelength ratios.

Urban also describes certain effects produced if the radiating elements in loudspeaker line arrays produce radial wave fronts instead of pure, flat wave fronts. He models this as a stack of slightly curved sources. Section 7 of the present paper examines the polar response of this stack and shows that grating lobes obtain at high frequency or large curvature.

Finally, it is important to examine how closely the mathematical models developed in this paper estimate the performance of loudspeaker line arrays. Section 8 compares modeled and measured polar response curves of three loudspeaker line arrays. Despite the vagaries of real-life sources and measurement challenges, the models provide remarkably good estimates of array performance over a wide frequency range. Button [20] and Engebretson [21] compare measured results against predictions produced by models similar to the ones developed in the present paper. Section 8 takes measured results from Engebretson and compares them directly against predictions produced explicitly by the straight-line source and arc source models developed in the following sections.

### 3 STRAIGHT LINE SOURCES

#### 3.1 Directivity Function of Straight Line Sources - General Form

A line source can be modeled as a continuum of infinitely small line segments distributed along a line. The acoustic pressure radiated from a line source<sup>(3)</sup> is

$$p = \int_{-l/2}^{l/2} \frac{A(l)e^{-j[kr(l)+\phi(l)]}}{r(l)} dl$$

<sup>1</sup> "Transition" distance is used instead of "critical" distance to avoid confusion with the term "critical distance" used in architectural acoustics where it refers to the distance at which the direct and reverberant fields are equal in level. See Eargle, J., Handbook of Sound System Design, ELAR Publishing Co., Commack, New York, 1989.

<sup>2</sup> The term "progressive" is used in the present paper instead of "spiral" originally used by the author. The term "spiral array" is sometimes used in reference to so-called "barber pole" arrays, as in Klepper [1].

<sup>3</sup> The time-varying factor  $e^{i\omega t}$  is omitted.

where  $L$  is the length of the line source,  $A(l)$  is the amplitude function along the line,  $\varphi(l)$  is the phase function along the line,  $k$  is the wave number and  $r(l)$  is the distance from any segment  $dl$  along the line to the point of observation  $\mathbf{P}$ .

The evaluation of this expression is simplified if we assume that the observation point  $\mathbf{P}$  is a large distance away. That is, that the distance is much greater than the length of the source and the distances to  $\mathbf{P}$  from any two segments along the line are approximately equal. This allows us to bring the  $r(l)$  term in the denominator to the front of the integral since, by definition,

$$\frac{1}{r(l/2)} \approx \frac{1}{r(-l/2)} \approx \frac{1}{r}.$$

Conversely, the  $r(l)$  term in the exponential has a significant influence on the directivity function. This is because the relatively small distance differences to  $\mathbf{P}$  from any two segments are not small compared to a wavelength, particularly at high frequency. Figure 1 shows that  $r(l)$  in the exponent can be expressed as

$$r(l) = l \sin \alpha$$

where  $\alpha$  is the angle between a line bisecting the source and a line from the midpoint of the source to  $\mathbf{P}$ . Substituting, the far field pressure at angle  $\alpha$  of a line source is

$$p(\alpha) = \frac{1}{r} \int_{-l/2}^{l/2} A(l) e^{-j[kl \sin \alpha + \varphi(l)]} dl.$$

The directivity function  $R(\alpha)$  of a line source is the magnitude of the pressure at angle  $\alpha$  over the magnitude of the maximum pressure that can be obtained. That is:

$$R(\alpha) = \frac{|p(\alpha)|}{|p_{\max}|}.$$

The maximum radiated pressure is obtained when all segments along the line radiate in phase, i.e. the exponential function equals unity<sup>(4)</sup>. It is given as

$$p_{\max} = \frac{1}{r} \int_{-l/2}^{l/2} A(l) dl.$$

The general form of the far field directivity function  $R(\alpha)$  of a line source is then

$$R(\alpha) = \frac{\left| \int_{-l/2}^{l/2} A(l) e^{-j[kl \sin \alpha + \varphi(l)]} dl \right|}{\left| \int_{-l/2}^{l/2} A(l) dl \right|}.$$

### 3.2 Directivity Function of Straight Line Sources - Uniform Amplitude and Phase

The general form of the straight-line source directivity function developed in Section 3.1 is valid for any amplitude and phase functions along the length of the line source. A *uniform* line source has constant amplitude and zero phase shift along its length, that is,  $A(l) = A$  and  $\varphi(l) = 0$ . Substituting into the general form yields an expression for the directivity function of a uniform line source  $R_U(\alpha)$ :

$$R_U(\alpha) = \frac{1}{L} \left| \int_{-l/2}^{l/2} e^{-jkl \sin \alpha} dl \right|.$$

Solving the integral and applying Euler's identities, this becomes

$$R_U(\alpha) = \frac{\sin(\frac{kL}{2} \sin \alpha)}{\frac{kL}{2} \sin \alpha}$$

or in terms of wavelength instead of frequency

$$R_U(\alpha) = \frac{\sin(\frac{\pi L}{\lambda} \sin \alpha)}{\frac{\pi L}{\lambda} \sin \alpha}.$$

Figure 2 shows polar response curves<sup>(5)</sup> of a uniform line source at various ratios of source length and wavelength. The polar response is wide at low ratios of  $L/\lambda$ . As the ratio is increased the directivity pattern narrows and exhibits nulls and lobes. These are explored in more detail in Section 3.3.

### 3.3 Lobes and Nulls – Uniform Straight Line Source

Figure 2 shows that at long wavelengths ( $\lambda > L$ ) the polar response of a uniform straight-line source is fairly omni-directional. At shorter wavelengths lobes and nulls are obtained. The position and magnitude of these are easily calculated.

<sup>5</sup> A polar response curve is the directivity function expressed in decibels and plotted on a polar chart. The on-axis pressure is used as the reference pressure, i.e.

$$\text{Polar response} = 20 \text{Log} \frac{R(\alpha)}{R(0)}.$$

<sup>4</sup> Note that the maximum pressure at any given distance and frequency may never actually be obtained.

The far field directivity function of a uniform line source is given in Section 3.2 as

$$R_V(\alpha) = \frac{\sin(\frac{\pi L}{\lambda} \sin \alpha)}{\frac{\pi L}{\lambda} \sin \alpha}.$$

This function has the generic form of  $\sin(z)/z$ . To evaluate this function on axis, that is  $z = 0$ , we must use L'Hospital's rule taking derivatives of the numerator and denominator. This yields

$$\lim_{z \rightarrow 0} \frac{\sin z}{z} \rightarrow \cos(0) = 1.$$

The fact that the limit approaches unity indicates that there will always be a maximum on-axis. Off-axis nulls are obtained when  $\sin(z)/z$  goes to zero. This occurs where the argument  $z$  reaches (non-zero) multiples of  $\pi$ . Substituting the full expression for  $z$ , nulls are obtained when

$$\frac{\pi L}{\lambda} \sin(\alpha) = m\pi$$

where  $m$  is a non-zero integer. Therefore, nulls are obtained at

$$|\sin(\alpha)| = m \frac{\lambda}{L} \quad \text{where } m = 1, 2, 3, \dots$$

Off-axis lobes of the directivity function are found in-between the nulls, that is, at

$$|\sin(\alpha)| = \frac{3\lambda}{2L}, \frac{5\lambda}{2L}, \frac{7\lambda}{2L}, \dots$$

This can be written as

$$|\sin(\alpha)| = \frac{(m + \frac{1}{2})\lambda}{L} \quad \text{where } m = 1, 2, 3, \dots$$

Finally, it is possible to calculate the amplitude of the lobes of a uniform line source. Since the amplitude decreases inversely with  $z$ , the pressure amplitude of the  $m^{\text{th}}$  lobe is

$$A_m = \left| \frac{\cos(m\pi)}{m\pi + \frac{\pi}{2}} \right| \quad \text{where } m = 1, 2, 3, \dots$$

### 3.4 Quarter-power Angle – Uniform Straight Line Source

Often it is useful to determine the -6dB angle of a uniform straight-line source. This is accomplished by

setting the generic form of the directivity function equal to  $0.5^{(6)}$  i.e.

$$\frac{\sin z}{z} = 0.5.$$

Solving numerically,  $z = 1.895$ . The -6dB point on one side of the central lobe is at angle  $\alpha$  where

$$z = 1.895 = \frac{\pi L}{\lambda} \sin \alpha.$$

The quarter-power angle is the total included angle between the -6dB points on either side of the central lobe and is given by

$$\theta_{-6dB} = 2\alpha.$$

Solving for  $\alpha$  in terms of length and wavelength and substituting we have

$$\begin{aligned} \theta_{-6dB} &= 2 \sin^{-1} \frac{1.895\lambda}{\pi L} \\ &\approx 2 \sin^{-1} \frac{0.6\lambda}{L} \end{aligned}$$

The quarter-power angle as a function of  $L/\lambda$  is shown in Figure 3. A similar result is obtained by Benson [22].

At small  $L/\lambda$ , i.e. a short line source and long wavelength, the quarter-power angle is wide. At large ratios of  $L/\lambda$ , i.e. long sources and short wavelengths, the quarter-power angle is narrow. For small angles<sup>(7)</sup>, where  $\sin(z) \approx z$ , the line source quarter-power angle is

$$\theta_{-6dB} = \frac{1.2\lambda}{L}$$

where  $\theta$  is in radians. Expressing  $\theta$  in degrees, we have

$$\theta_{-6dB} = 68.8 \frac{\lambda}{L} \text{ (degrees)}.$$

In some cases, it is convenient to use frequency rather than a ratio of wavelength and source length. Rewriting, the quarter-power angle equation for uniform line sources becomes (approximately)

$$\theta_{-6dB} \approx \frac{2.4 \cdot 10^4}{fL} \quad (L \text{ in meters, } f \text{ in Hz})$$

<sup>6</sup> The directivity function is a pressure ratio. A pressure ratio of .5 yields a sound pressure level difference of -6dB.

<sup>7</sup> The small angle approximation holds for angles less than about 30 degrees. Note that  $\sin(\pi/6) = 0.5000$  and  $\pi/6 = 0.5235$  so that the error is less than 5%.

or

$$\theta_{-6dB} \approx \frac{7.8 \cdot 10^4}{fL} \quad (L \text{ in feet, } f \text{ in Hz}).$$

The *directivity response* of a line source is a plot of the quarter power angle versus frequency. The directivity response of uniform line sources of several lengths is shown in Figure 4. These show that the quarter-power angle of large sources is quite narrow at high frequency. For instance, at 10kHz a 4-meter long uniform straight-line source has a -6dB angle of 0.6 degrees.

### 3.5 On-axis Pressure Response of Straight Line Sources

The on-axis pressure response of a line source is derived in much the same manner as the directivity function. The pressure radiated from each infinitely small line segment is summed at an observation point  $\mathbf{P}$ . In this case, however,  $\mathbf{P}$  is at a distance  $x$  along an axis normal to the source and no far field assumptions are taken.

#### 3.5.1 Conventional Approach - Midpoint Method

Figure 5 shows the conventional geometric construction used to solve for the pressure along a path normal to the source, beginning at its midpoint. Referring to Figure 5,  $L$  is the total length of the source and  $r_{mid}$  is the distance from any radiating element  $dl$  of the source to any distance  $x$  along the horizontal axis. The general form for the radiated pressure at  $x$  is

$$p_{mid}(x) = \int_{-L/2}^{L/2} \frac{A(l)e^{-j[kr_{mid}(x,l)+\varphi(l)]}}{r_{mid}(x,l)} dl$$

where

$$r_{mid}(x,l) = \sqrt{x^2 + l^2}$$

The pressure response is the logarithmic ratio of the magnitude of the pressure squared at  $x$  over the magnitude of the pressure squared at some reference distance, i.e.

$$R(x) = 20 \log \frac{|p(x)|}{|p(x_{ref})|}.$$

The on-axis pressure response of a 4-meter uniform straight line source, where  $A(l)=A$  and  $\varphi(l)=0$ , at 8kHz is shown in Figure 6. The pressure response generally decreases at a rate of -3dB per doubling of distance out to approximately 100 meters. It exhibits undulations in this region, the magnitudes of which increase as the distance approaches 100 meters. Beyond 100 meters, the pressure amplitude no longer undulates and decreases monotonically at -6dB per doubling of distance. The point at which this change occurs is referred to as the *transition distance*. The region between the source and

the transition distance is referred to as the near field and the region beyond is the far field.

The transition distance varies with source length and frequency. Figure 7 shows the on-axis response of three different length uniform line sources at 8kHz. As length  $L$  increases, the transition distance increases. Figure 8 shows the on-axis response of a 4-meter long uniform line source at 500Hz, 2kHz, and 8kHz. It shows that the transition distance also increases with frequency.

#### 3.5.2 Midpoint versus Endpoint

The conventional approach used to determine the on-axis pressure response of a line source discussed in Section 3.5.1 is to take a path normal to the source beginning at its midpoint. This yields a result, however, that is unique to this path. Choosing the midpoint as the initial point introduces symmetry into the analysis and minimizes the apparent aperture of the source. If a different initial point is chosen, the line source appears longer on one side of this point than on the other side. This difference is maximized when the endpoint of the source is chosen. In this case, the source has a length  $L$  in one direction and zero length in the other. If the on-axis pressure is summed along a path normal to the source beginning at the endpoint of the line source, the transition distance moves increases substantially.

Figure 9 shows a modified geometric construction for calculating the on-axis pressure response. The pressure summed along a path normal to the endpoint of a line source is

$$p_{end}(x) = \int_{-L/2}^{L/2} \frac{A(l)e^{-j[kr_{end}(x,l)+\varphi(l)]}}{r_{end}(x,l)} dl$$

where

$$r_{end}(x,l) = \sqrt{x^2 + \left(l + \frac{L}{2}\right)^2}.$$

Figure 10 compares the on-axis response of a 4-meter long uniform straight-line source, where  $A(l)=A$  and  $\varphi(l)=0$ , at 8kHz using the midpoint and endpoint methods. The last peak of the midpoint near field response occurs at approximately 100 meters. The last peak of the endpoint response occurs at approximately 400 meters. Note that the endpoint response is at a lower amplitude level than the midpoint response in the near field. In the far field the curves converge and yield the monotonically -6dB per doubling of distance decrease described above.

If the origin of the path is moved beyond the endpoint, the distance to the last peak occurs at greater and greater distances. It can be shown that the distance to the far field continues to increase as one chooses a path further off the midpoint axis. However, the pressure levels fall off quite dramatically once the endpoint is breached. This is shown in Figure 11. The first two curves labeled "0" and "L/2" are the midpoint and endpoint pressure responses, respectively, shown in Figure 10. The next two curves are on-axis pressure response curves

beginning at points one length ( $L$ ) and three-halves lengths ( $3L/2$ ) vertically displaced from the midpoint.

The curves in Figure 11 are slices through the pressure field, normal to the source, at increasing displacement from the midpoint. We can see that as the origin of the path is moved off the midpoint, the amplitude levels of the pressure decreases in the near field. It is approximately  $-6\text{dB}$  at the endpoint, but decreases to around  $-40\text{dB}$  at  $L$  and  $3L/2$ . Also, the pressure response curves  $L$  and  $3L/2$  undulate in a fashion that in the aggregate is nearly flat from the source to the far field.

The  $L$  and  $3L/2$  response curves are so low in level relative to the midpoint response that they are of limited significance. However, the endpoint curve ( $L/2$ ) is a material feature of the pressure field. It is approximately  $-6\text{dB}$  down from the midpoint response and undulates well past the midpoint transition distance. The fact that two such disparate response curves can be obtained by merely shifting the origin of the normal path demonstrates the ambiguity of the term ‘‘on-axis response.’’

### 3.6 Pressure Field of Straight Line Sources

The most comprehensive approach to observe the pressure response of a line source is to compute its *pressure field*. This eliminates the question of midpoint versus endpoint. It is obtained by rewriting the expression for the radiated pressure in terms of Cartesian coordinates as setup in Figure 12. The pressure at any point  $\mathbf{P}$  is

$$p(x, y) = \int_{-\frac{1}{2}}^{\frac{1}{2}} \frac{A(l)e^{-j[kr(x, y, l) + \varphi(l)]}}{r(x, y, l)} dl$$

where

$$r(x, y, l) = \sqrt{x^2 + (y - l)^2}$$

Figure 13 shows the pressure field of a 4-meter uniform straight line source, where  $A(l)=A$  and  $\varphi(l)=0$ , in several frequency bands. The major on-axis lobe gets narrower with increasing frequency as expected. The minor lobes increase in number and lower amplitude levels. At high frequency they dissolve into very complex patterns of constructive and destructive interference. Note that the pressure varies across the major lobe at 8kHz in a manner consistent with the pressure slices shown in Figure 11. The undulations extend to a greater distance from a line normal to the endpoint than from the midpoint.

## 4 ARC SOURCES

Many loudspeaker line arrays used in practice are actually curved. This is because pure straight-line arrays at high frequency produce a narrow vertical polar response – often too narrow to reach audiences beneath and slightly in front of the array. A slightly curved array provides superior coverage in this area. One important type of a curved line source is an arc source.

An arc source is comprised of radiating elements arranged along a segment of a circle. At all frequencies it

provides a wider directivity response than a straight-line source of the same length. At high frequency, it provides a polar pattern that corresponds to the included angle of the arc.

### 4.1 Polar Response of Arc Sources

The derivation of the directivity function of an arc source follows the same steps described above for a straight-line source. Figure 14 shows the geometric construction of an arc source with radius  $R$  and total included angle  $\theta$ . The pressure radiated by an arc at off-axis angle  $\alpha$  is

$$p_A(\alpha) = \int_{-\frac{\theta}{2}}^{\frac{\theta}{2}} \frac{A(\phi)e^{-j[kr_A(\phi, \alpha) + \varphi(\phi)]}}{r_A(\alpha, \phi)} R d\phi.$$

As in Section 3.1, the evaluation of this expression is simplified if we assume that the observation point  $\mathbf{P}$  is a large distance away. In this case, the distance is much greater than the length of the arc and the distances to  $\mathbf{P}$  from any two segments along the arc are approximately equal. This allows us to bring the  $r_A$  term in the denominator to the front of the integral since by definition

$$\frac{1}{r_A(\theta/2)} \approx \frac{1}{r_A(-\theta/2)} \approx \frac{1}{r_A}.$$

Conversely, the  $r_A$  term in the exponential has a significant influence on the directivity function. This is because the relatively small distance differences to  $\mathbf{P}$  from any two segments are not small compared to a wavelength. Figure 14 shows that  $r_A$  in the exponent can be expressed as

$$r_A(\alpha, \phi) = 2R \sin\left[\frac{\phi}{2}\right] \sin\left[\frac{\phi}{2} + \alpha\right]$$

where  $\alpha$  is the angle between a line that bisects the arc angle and a line from the center point of the arc to  $\mathbf{P}$ . Substituting, the far field directivity function of an arc is then expressed in general form as

$$R_A(\alpha) = \left| \frac{\int_{-\frac{\theta}{2}}^{\frac{\theta}{2}} A(\phi)e^{-j[kr_A(\alpha, \phi) + \varphi(\phi)]} R d\phi}{\int_{-\frac{\theta}{2}}^{\frac{\theta}{2}} A(\phi) R d\phi} \right|.$$

If we assume constant amplitude and zero phase shift along the arc, i.e.  $A(\phi) = A$  and  $\varphi(\phi) = 0$ , the directivity function reduces to<sup>(8)</sup>:

<sup>8</sup> This integral does not have a convenient closed form solution similar to the one obtained for the line array. Wolff and Malter provide a point source summation version of the directivity function as follows:

$$R_A(\alpha) = \frac{1}{R\theta} \left| \int_{-\theta/2}^{\theta/2} e^{-jkr_A(\alpha, \phi)} R d\phi \right|$$

where  $r_A$  is expressed above. The polar response curves of a uniform  $60^\circ$  arc source at various ratios of radius and wavelength are shown in Figure 15. Generally, these are wide for low ratios of  $R/\lambda$  and approach the included angle of the arc at higher ratios.

## 4.2 On-Axis Pressure Response of Arc Sources

The on-axis pressure response of an arc source can be expressed in a form similar to the earlier expressions for straight-line sources. Figure 16 shows the geometric construction of an arc source with radius  $R$  and total included angle  $\theta$ . The pressure of an arc source at distance  $x$  is

$$p_A(x) = \int_{-\theta/2}^{\theta/2} \frac{A(\phi) e^{-j[kr_A(x, \phi) + \phi(\phi)]}}{r_A(x, \phi)} R d\phi$$

where

$$r_A(x, \phi) = \sqrt{(x + R(1 - \cos\phi))^2 + R^2 \sin^2\phi}.$$

Figure 17 provides a comparison of the pressure response of equivalent length uniform straight line and arc sources. Though the arc source is curved only 30 degrees, its on-axis response is materially smoother in the near field than the one produced by the straight-line source.

Like a line source, the pressure response of an arc source changes with arc length and frequency. Figure 18 shows the on-axis response of three uniform arc sources of various lengths. The different lengths are provided by a constant radius (4m) with an adjusted included angle. Figure 19 shows how the pressure response changes with frequency. Note that the transition from the near field to the far field is generally smoother for an arc than for a line source at all lengths and frequency.

## 4.3 Pressure Field of Arc Sources

The two-dimensional pressure field of an arc source is given by

$$R(\alpha) = \frac{1}{2m+1} \left[ \sum_{n=-m}^{n=m} \cos \left[ \frac{2\pi R}{\lambda} \cos(\alpha + n\phi) \right] + i \sum_{n=-m}^{n=m} \sin \left[ \frac{2\pi R}{\lambda} \cos(\alpha + n\phi) \right] \right]$$

where  $m$  is an integer,  $2m+1$  is the number of point sources, and  $\phi$  is the angle subtended between any two adjacent point sources.

$$p_A(x, y) = \int_{-\theta/2}^{\theta/2} \frac{A(\phi) e^{-j[kr_A(x, y, \phi) + \phi(\phi)]}}{r_A(x, y, \phi)} R d\phi$$

where

$$r_A(x, y, \phi) = \sqrt{(x + R(1 - \cos\phi))^2 + (y - R \sin\phi)^2}$$

The geometric construction is shown in Figure 20. Figure 21 shows the pressure field of a uniform arc source, where  $A(\phi)=A$  and  $\phi(\phi)=0$ , in several frequency bands. The response is quite different from that produced by a uniform straight-line source. At low frequency, a uniform arc source can produce either a lobe or a null on-axis. At mid and high frequency a wedge pattern is produced that corresponds to the included angle of the arc.

## 5 J-SOURCES

A J-source is comprised of a line source and an arc source. Generally, the straight segment is located above the arc segment and is intended to provide the long throw component of the polar response. The arc segment is intended to provide coverage in the area below and in front of the source. Together the segments provide an asymmetric polar response in the vertical plane.

### 5.1 Polar Response of J-Sources

The directivity function of a J-source is obtained by combining the directivity functions of the line and arc sources presented in previous sections. The geometric construction is shown in Figure 22 where  $L$  is the length of the straight segment and  $R$  and  $\theta$  specify the arc segment. We assume that the straight and arc segments are adjacent and that the center point of the arc is on a line perpendicular to the straight segment through its lower endpoint.

If we choose the center point of the line segment as the origin, then the pressure radiated from the line segment in the far field at off-axis angle  $\alpha$  is

$$p_L(\alpha) = \frac{1}{r} \int_{-\theta/2}^{\theta/2} A_L(l) e^{-j[kr_L(\alpha, l) + \phi_L(l)]} dl$$

where

$$r_L(\alpha, l) = l \sin(\alpha)$$

as shown in Section 3.1. Here,  $A_L(l)$  and  $\phi_L(l)$  are the amplitude and phase functions of the line segment. Now, since we must rotate the arc segment by  $\theta/2$  relative to the horizontal, we will also change the limits of integration. The pressure radiated in the far field from the rotated arc source is

$$R_A(\alpha) = \frac{1}{r} \int_0^\theta A_A(\phi) e^{-j[kr_A(\alpha, \phi) + \phi_A(\phi)]} R d\phi.$$

where

$$r_A(\alpha, \phi) = 2\mathbf{R} \sin\left[\frac{\phi}{2}\right] \sin\left[\frac{\phi}{2} + \alpha\right]$$

and  $A_A(\phi)$  and  $\varphi_A(\phi)$  are the amplitude and phase functions of the arc segment. To properly sum the radiated pressure from the line and arc segments, a new function is required to express the relative distance difference between them. Referring to Figure 22, it is given as

$$r_J(\alpha) = \frac{L}{2} \sin(\alpha).$$

The general form for the radiated pressure in the far field of a J-source is then

$$p_J(\alpha) = \frac{1}{r} \left[ \int_{-\frac{1}{2}}^{\frac{1}{2}} A_L(l) e^{-j[kr_L(\alpha, l) + \varphi_L(\phi)]} dl + \int_0^\theta A_A(\phi) e^{-j[kr_A(\alpha, \phi) + \varphi_A(\phi) + r_J(\alpha)]} \mathbf{R} d\phi \right]$$

If we assume that the amplitudes per-unit-length are uniform over the line and arc segments, and that the phase shifts are zero, the relative source strengths are proportional to their relative lengths. Letting  $A_L$  and  $A_A$  be the constant amplitudes-per-unit length of the line and arc segments respectively, the directivity function of a J-source reduces to

$$R_J(\alpha) = \frac{1}{A_L L + A_A \mathbf{R} \theta} \left[ A_L \int_{-\frac{1}{2}}^{\frac{1}{2}} e^{-jkr_L(\alpha, l)} dl + A_A \int_0^\theta e^{-j[kr_A(\alpha, \phi) + r_J(\alpha)]} \mathbf{R} d\phi \right]$$

The contributions of the line segment and the arc segment to the polar response of a uniform J-source are shown in Figure 23. As expected, the line segment provides long throw and the arc segment provides a relatively wide angle of coverage rotated downward. The response of the J-source is a blend of the two.

The polar response of a J-source changes with the length of the line segment, the radius and included angle of the arc segment, the relative amplitudes of the two segments, and frequency. Figure 24 shows polar response curves of a J-source with a two-meter long line segment, a one-meter radius, a 60° included angle and equal amplitudes-per-unit-length. The polars show that the straight segment of the J-source dominates the response and produces a very narrow beam, particularly at high frequency. The arc segment does not fully balance the high gain of the straight segment.

There are several approaches to providing a more balanced response. One is to make the straight segment shorter thereby reducing the gain. A second is to increase  $A_A$  relative to  $A_L$ . For instance, one might use a J-source that has a one-meter long straight segment (as opposed to 2-meter in the previous example) and set  $A_A = 2A_L$  (instead of  $A_A = A_L$ ). The polar response of this modified J-source is considerably more balanced than the uniform J-source as shown in Figure 25.

## 5.2 On-Axis Pressure Response J-Sources

The on-axis pressure response of a J-source is obtained by combining the pressure response functions of the line and arc sources presented above. The geometric construction is shown in Figure 26 where  $L$  is the length of the straight segment and  $\mathbf{R}$  and  $\theta$  specify the arc segment. Note that the lower endpoint of the arc segment is taken as the initial point for the on-axis response. Based on this geometry, the pressure radiated at point  $\mathbf{P}$  from a J-source is

$$p_J(x) = \int_0^L \frac{A_L(l) e^{-j[kr_L(x, l) + \varphi_L(\phi)]}}{r_L(x, l)} dl + \int_0^\theta \frac{A_A(\phi) e^{-j[kr_A(x, \phi) + \varphi_A(\phi)]}}{r_A(x, \phi)} \mathbf{R} d\phi$$

where

$$r_L(x, l) = \sqrt{x^2 + (\mathbf{R} \sin \theta + l)^2}$$

and

$$r_A(x, \phi) = \sqrt{(x + \mathbf{R}(1 - \cos \phi))^2 + \mathbf{R}^2 (\sin \theta - \sin \phi)^2}$$

Figure 27 compares the on-axis pressure response of uniform equivalent-length straight line and J-sources, where  $A(\phi) = A$ . The straight segment of the J-source dominates the response, producing undulations in the near field very similar to those of the straight-line source. However, the on-axis aperture of the J-source is foreshortened relative to the equal-length line source so the distance to the far field is marginally shorter.

## 5.3 Pressure Field of J-Sources

The geometric construction for the pressure field of a J-source is shown in Figure 28. The general form for the pressure at  $\mathbf{P}$  is

$$p_J(x, y) = \int_0^L \frac{A_L(l) e^{-j[kr_L(x, y, l) + \varphi_L(\phi)]}}{r_L(x, y, l)} dl + \mathbf{R} \int_0^\theta \frac{A_A(\phi) e^{-j[kr_A(x, y, \phi) + \varphi_A(\phi)]}}{r_A(x, y, \phi)} d\phi$$

where

$$r_L(x, y, l) = \sqrt{x^2 + (y + l)^2}$$

and

$$r_A(x, y, \phi) = \sqrt{(x + R(1 - \cos \phi))^2 + (y + L + R \sin \phi)^2}$$

The pressure field of a uniform J-source, where  $A(\phi)=A$  and  $\varphi(\phi)=0$  in several frequency bands is shown in Figure 29. The parameters of the J-source are the same as those used for the modified J-source as described in Section 5.1, i.e. a one-meter straight segment and  $A_A = 2A_L$ . These plots show clearly that a J-source is a blend of straight and arc sources. This is particularly true at mid and high frequency where the constituent responses are easily identifiable.

## 6 PROGRESSIVE SOURCES

Like a J-source, a progressive source provides an asymmetric polar response in the vertical plane. However, unlike a J-source it is a continuous curve rather than two distinct segments. The curvature increases with distance along the curve. This results in an upper portion that is largely straight and a lower portion that is curved downward.

### 6.1 Polar Response of Progressive Sources

There are numerous possible mathematical expressions for progressive expansions, each providing different rates of curvature. The relevant set of expressions for loudspeaker arrays is characterized by curvature changes at equal intervals of length along the progressive curve. The interval corresponds to the height of a single loudspeaker enclosure of the array.

An *arithmetic* progressive source is one for which the angle between successive enclosures changes by a predetermined angle given by  $(n-1)\Delta\theta$  where  $n$  is the  $n$ th enclosure and  $1 < n < N$  where  $N$  is the total number of enclosures in the array. For example, if  $\Delta\theta=1^\circ$  and the first enclosure is hung at  $0^\circ$  (horizontal), the second enclosure would be hung at  $1^\circ$  relative to the first enclosure and the third at  $2^\circ$  relative to the second enclosure. This defines a progressive curve where the aiming angle of the  $n$ th enclosure is oriented to the horizontal axis by  $0^\circ, 1^\circ, 3^\circ, 6^\circ, 10^\circ$ , and so on - an arithmetic expansion. An incremental angle  $\Delta\theta$  of  $2^\circ$  would yield  $0^\circ, 2^\circ, 6^\circ, 12^\circ$  and,  $20^\circ$ . The terminal angle  $\Omega$  of an array, i.e. the aiming angle relative to the horizontal of the last enclosure, is given by

$$\Omega = \frac{1}{2} N(N+1)\Delta\theta$$

where  $N$  is the total number of enclosures. The total length of the source is

$$L = NH$$

where  $H$  is the height of a single enclosure. These two terms,  $\Omega$  and  $L$ , fully define an arithmetic progressive source.

The far field directivity function of an arithmetic progressive source is derived in the same manner used earlier for the line, arc, and J sources. The pressure radiated along the source is summed at a point  $\mathbf{P}$  in the far field. The shape of the polar response curves will be determined primarily by the small distance function  $r_s$ .

The first step is to express the progressive as a continuum of small radiating segments of length  $\Delta L$ .  $\Delta L$  should be chosen to be a small fraction of the shortest wavelength of interest. As a practical guideline,  $\Delta L$  should be set approximately equal to one-quarter of a wavelength, that is,

$$\Delta L = \frac{\lambda}{4}.$$

The total number of segments is then

$$M = \frac{L}{\Delta L}$$

and the incremental angle between the elements is

$$\Delta\psi = \frac{2\Omega}{M(M+1)}.$$

The progressive source can then be expressed in parametric form as

$$x(\sigma) = \sum_{\eta=0}^{\sigma} -\sin\left[\frac{1}{2}\eta(\eta+1)\Delta\psi\right]\Delta L$$

and

$$y(\sigma) = \Delta L + \sum_{\eta=0}^{\sigma} -\cos\left[\frac{1}{2}\eta(\eta+1)\Delta\psi\right]\Delta L.$$

The geometric construction of an arithmetic progressive source is shown in Figure 30. Its far field directivity function is

$$R_s(\alpha) = \frac{\left| \sum_{\sigma=0}^M A_\sigma e^{-j[kr_s(\sigma, \alpha) + \varphi_\sigma]} \right|}{\left| \sum_{\sigma=0}^M A_\sigma \right|}.$$

where

$$r_s(\sigma, \alpha) = \sin\left[\alpha - \tan^{-1}\left(\frac{x(\sigma)}{y(\sigma)}\right)\right] \sqrt{x(\sigma)^2 + y(\sigma)^2}$$

The far field directivity function for a uniform progressive source, where  $A_\sigma = A$  and  $\varphi_\sigma = 0$ , is

$$R_S(\alpha) = \frac{1}{M+1} \left| \sum_{\sigma=0}^M e^{-jkr_S(\sigma, \alpha)} \right|$$

where  $r_S$  is given above. The polar response of a uniform arithmetic progressive source is remarkably constant with frequency. Figure 31 shows the polar response curves of a 5-meter long progressive source with a terminal angle of  $45^\circ$ .

## 6.2 On-Axis Pressure Response Progressive Sources

The geometric construction for the on-axis pressure response of a progressive source is shown in Figure 32. The pressure response along a path from the lower end is

$$p_S(x) = \sum_{\sigma=0}^M A_\sigma \frac{e^{-j[kr_S(x, \sigma) + \theta_\sigma]}}{r_S(x, \sigma)}$$

where

$$r_S(x, \sigma) = \sqrt{(x - x(\sigma))^2 + (y(M) - y(\sigma))^2}.$$

Figure 33 compares the on-axis response curves of equivalent length *uniform* straight-line and progressive sources. These curves show that the progressive source has reduced undulations in the near field and a smoother transition from the near field to the far field.

## 6.3 Pressure Field of Progressive Sources

The geometric construction for the pressure field of a progressive source is shown in Figure 34. The pressure at any point **P** is

$$p_S(x, y) = \sum_{\sigma=0}^M A_\sigma \frac{e^{-j[kr_S(x, y, \sigma) + \theta_\sigma]}}{r_S(x, y, \sigma)}$$

where

$$r_S(x, y, \sigma) = \sqrt{(x - x(\sigma))^2 + (y - y(\sigma))^2}.$$

The pressure field of a uniform progressive source in several frequency bands is shown in Figure 35. These results illustrate the well-behaved asymmetrical response of a progressive source that makes them an excellent geometry upon which to base loudspeaker arrays for sound reinforcement applications.

## 7 ADVANCED TOPICS

As a practical matter, large line arrays of loudspeakers are not perfectly continuous line sources. For instance, they may have gaps in between the loudspeaker enclosures due to enclosure construction material or

spacing. These gaps are effectively non-radiating portions of the line and may have an effect on the performance of the array. Also, certain radiating elements in loudspeaker line arrays may produce radial wave fronts instead of pure, flat wave fronts. This may also have an effect on the performance of the array. These topics are analyzed in the following sections.

### 7.1 Gaps in Line Sources

In previous sections, we assume that each type of line source entire length is continuous along its entire length. In practice, however, it may not be possible to achieve this. For instance, the thickness of the material used to construct a loudspeaker enclosure does not radiate acoustic energy. When loudspeaker enclosures are stacked into an array, these non-radiating segments are distributed along the length of the array. This can be modeled by limiting the integration of the line source to the radiating portions only. Referring to Figure 36,  $d$  is the dimension of the non-radiating element on either side of the radiating element.

The directivity function of a line source with  $N$  elements of length  $L$  and gaps between them is

$$R(\alpha) = \sum_1^N \frac{\left| \int_{(N-1)L+d}^{NL-d} A(l) e^{-j[kl \sin \alpha + \phi(l)]} dl \right|}{\left| \int_{(N-1)L+d}^{NL-d} A(l) dl \right|}.$$

In general, gaps have very little effect on the primary lobe but change the structure of the off-axis lobes and nulls. Figure 37 shows the linear polar response<sup>9</sup> of a four-element uniform line source with gaps. The graphs show the effects of changing the radiating percentage from 100% to 90%, 75% and 50%. At low frequency, where the gap length is a small fraction of the wavelength, gaps have very little effect. At high frequency, the side lobe structure changes materially with gap length. The lobes get wider and change position.

Contemporary loudspeaker line array enclosures are usually designed to maximize the radiating percentage. If an enclosure is .5 meters high and constructed out of typical materials, radiating percentages can exceed 90%. However, if the spacing between enclosures gets large, gaps may exceed this threshold and the polar response will be affected.

### 7.2 Stack of Arc Sources vs. Line Sources

In practice, certain components of a loudspeaker system may produce wave fronts that are curved instead of perfectly straight. When stacked in an array, these may more closely resemble a stack of arc sources rather than a continuous straight-line source. Figure 38 shows a stack of three arc sources representing an array of three loudspeaker components with radial wave fronts. The

<sup>9</sup> Linear polar response is a rectilinear representation of the polar response, i.e. dB along the y-axis and angle along the x-axis.

effects that radial wave fronts have on the directivity function can be estimated by summing the radiation from a stack of arc sources.

As derived in Section 4.1, the directivity function of a uniform arc source is

$$R_A(\alpha) = \frac{1}{R\theta} \left| \int_{-\theta/2}^{\theta/2} e^{-jkr_A(\phi, \alpha)} R d\phi \right|$$

where

$$r_A(\phi, \alpha) = 2R \sin \left[ \frac{\phi}{2} \right] \sin \left[ \frac{\phi}{2} + \alpha \right]$$

and  $R$  is the radius and  $\theta$  is the included angle of the arc. The directivity function of a stack of arc sources is obtained by applying the first product theorem<sup>(10)</sup>. In this case, the directivity function of the arc is multiplied by the directivity function of an array of simple sources. The far field directivity function for an array of  $N$  simple sources of equal amplitude and phase distributed a distance  $D$  apart along a line is given by

$$R_p(\alpha) = \frac{1}{N} \left| \sum_{n=1}^N e^{-j[k(n-1)D \sin \alpha]} \right|.$$

Applying the first product theorem, the directivity function of a vertical stack of arc sources is

$$R_{Ap}(\alpha) = R_A(\alpha) R_p(\alpha).$$

Figure 39 shows the effects of non-flat wave fronts on the directivity function of the sources, compared to a perfectly flat wave front. As with gaps in a line source, curvature primarily produces changes in the lobe/null structure of the off-axis response. The changes increase with increasing curvature and are more predominant when the curvature is a material fraction of a wavelength.

Figure 39a compares the directivity function of a uniform line source of length  $3L$  with an array of three curved sources of length  $L$ , where the curvature  $\delta$  of the arc is one-eighth wavelength. The directivity functions are very similar, with only small differences in the lobe/null structure. In particular, note that the nulls at approximately  $18^\circ$ ,  $35^\circ$  and  $60^\circ$  are not as deep with the stack of arc sources.

Figures 39b and 39c show the directivity functions of the uniform line and the three-element array at curvatures of  $\frac{1}{4}$  and  $\frac{1}{2}$  wavelengths. In these cases, lobes gradually replace the nulls at  $18^\circ$ ,  $35^\circ$  and  $60^\circ$ . At  $\frac{1}{4}$  wavelength, the lobe at  $18^\circ$  is approximately 10dB below the level of the on-axis lobe, up from approximately 20dB. This represents a practical limit to curvature that maintains,

generally speaking, the directivity function of a pure line source. The response at  $\frac{1}{2}$  wavelength is unacceptable as the  $18^\circ$  lobe is here nearly equal in amplitude to the primary lobe.

This  $\frac{1}{4}$  wavelength limit on curvature allows us to estimate, for a given curvature, the practical upper frequency limit for which it maintains the directivity response of a uniform line source. If a source has an element length  $L$  of 15 cm and a total arc angle of  $20^\circ$  then

$$\delta = \frac{L}{2} \tan \left( \frac{\theta}{4} \right) = .66cm$$

and the upper frequency limit is

$$f = \frac{c}{4\delta} \approx 13kHz.$$

Polar response curves of a stack of three 15cm high,  $20^\circ$  sources are shown in Figure 40. The data are superimposed over the polar response of a line source 45cm long. The  $20^\circ$  source tends to merge the third and fourth off-axis lobes. The amplitude of this merged lobe increases with frequency. At approximately 12.5kHz the lobes are 10dB below the primary on-axis lobe. This corresponds closely to the 13kHz estimate above.

## 8 APPLICATIONS

The mathematical models developed in the previous sections will provide useful estimates of the performance of many types of loudspeaker line arrays. However, the accuracy of the estimates may be compromised by several factors. First, real-life loudspeaker systems do not often behave like perfect sources. In addition to the gaps and radial wavefronts discussed in Section 8, other potential factors include cone or diaphragm breakup, suspension and magnetic non-linearities, and enclosure resonance and edge (diffraction) effects. Second, collecting far field data can be problematic since the microphone must be placed at large distances. Most anechoic chambers provide adequate distances to measure only relatively small arrays. Large arrays can be measured outdoors but environmental factors such as wind and atmospheric turbulence may affect results. Alternatively, data may be taken in a large indoor space but the acoustical characteristics of the room must be isolated and removed from the measurements. Nonetheless, despite all of these potential sources of errors, useful estimates can be produced as illustrated in the following sections.

### 8.1 Example 1: Small Straight Line Array – Low Frequency Model

The first example compares the modeled polar response of a small straight-line array against measured results. The array is comprised of six small horns stacked in a vertical array as shown in Figure 41. Each horn is approximately 8 inches tall resulting in an array 48 inches high. Polar data were collected on this array at a distance of 15 feet in an anechoic chamber. See Ureda [23].

<sup>10</sup> The first product theorem states that the directional factor of an array of identical sources is the product of the directional factor of the array and the directional factor of a single element of the array. See Kinsler, Frey, Coppens and Sanders "Fundamentals of Acoustics", forth edition, John Wiley and Sons, 1982.

The most straightforward approach to model this array is to assume that it is a uniform straight-line source. This assumption will hold at low frequency where the mouth is less than one wavelength high. Since this horn has a mouth<sup>11</sup> height of approximately 6.5 inches, the highest useable frequency of the model is approximately 2kHz. From Section 3.2, the directivity function of a uniform line source is

$$R_U(\alpha) = \frac{1}{L} \left| \int_{-L/2}^{L/2} e^{-jkl \sin \alpha} dl \right|$$

where in this case  $L = 48$  inches. Figure 42 shows measured versus modeled polar response. Note that the model assumes a sine wave input that yields a very fine lobe and null structure. The measured data are 1/3 octave pink noise that tends to fill the sharp nulls of a sine wave response. Nonetheless, the modeled response closely resembles the measured data. Note that the 1.5" gaps between the horn mouths do not materially affect the modeled performance.

## 8.2 Example 2: Small Straight Line Array – High Frequency Model

The polar response estimate of the six-horn array described in Section 8.1 can be extended to higher frequency if we use a stack of arc sources model instead of a uniform straight line. This is reasonable since the polar response of the individual horns will approach the vertical coverage angle at higher frequency. The horns have a vertical coverage angle of 20 degrees. Using the directivity function of a stack of uniform arc sources from Section 7.2 where

$$R_{AP}(\alpha) = R_A(\alpha)R_P(\alpha),$$

$$R_P(\alpha) = \frac{1}{N} \left| \sum_{n=1}^N e^{-j[k(n-1)D \sin \alpha]} \right|,$$

$$R_A(\alpha) = \frac{1}{R\theta} \left| \int_{-\theta/2}^{\theta/2} e^{-jkr_A(\phi, \alpha)} R d\phi \right|,$$

$$r_A(\phi, \alpha) = 2R \sin \left[ \frac{\phi}{2} \right] \sin \left[ \frac{\phi}{2} + \alpha \right]$$

and

$$R = \frac{L}{2 \sin \left( \frac{\theta}{2} \right)},$$

and setting  $N = 6$ ,  $L = 6.5''$ ,  $D = 8''$  and  $\theta = 20^\circ$  we obtain the polar response curves shown in Figure 43. Again, the curves are based on sine wave response and the measured data were collected in 1/3 octave bands of pink noise. Nonetheless, the model predicts the grating lobes at the higher frequencies.

## 8.3 Example 3: Large Curved Array

Engebretson [21] recently took polar response data on several large arrays. Among these was an eight element curved array. Each element is approximately 1/2 meter high resulting in a total length of four meters. Vertical polar data were derived from ground-plane MLSSA impulse measurements taken at 20 meters on 5-degree intervals. The data were taken inside a vacant airplane hangar to prevent wind-borne temperature gradients and other disturbances. Figure 44 shows the array of eight cabinets configured for ground plane measurement. The eight boxes are shown set on end with 5-degree splay angles between adjacent cabinets.

This array can be modeled as an arc source with an included angle of 40 degrees and an arclength of 4 meters. The polar response at standard 1/3-octave center frequencies can be estimated using the far field directivity function of a uniform arc source. From Section 4.1, this is

$$R_A(\alpha) = \frac{1}{R\theta} \left| \int_{-\theta/2}^{\theta/2} e^{-jkr_A(\alpha, \phi)} R d\phi \right|$$

where

$$R = \frac{L}{\theta}$$

and

$$r_A(\alpha, \phi) = 2R \sin \left[ \frac{\phi}{2} \right] \sin \left[ \frac{\phi}{2} + \alpha \right].$$

The modeled polar response curves are shown in Figure 45. The measured data from Engebretson are shown as dots superimposed on the modeled curves. Note that the measured data are at 5-degree increments – the directivity function provides continuous curves. We can see that the agreement between measured and modeled is quite reasonable. The large lobes along the sides of the polars may be due to diffraction effects or room effects. Neither of these effects is accounted for in the model. Nonetheless, the model provides a useful estimate of the polar response across more than six octaves.

## 9 SUMMARY

This paper provides mathematical models that estimate the performance of several types of loudspeaker line arrays. Specifically, models are provided to estimate the polar response, on-axis pressure response and pressure

<sup>11</sup> The horn is 8 inches tall but the mouth is only 6.5 inches because mounting flanges on either side of the mouth are 3/4 inches wide.

fields of straight, curved (arc), “J” and progressive arrays. The first few sections of the paper provide a review of uniform straight-line sources including derivations of the far field polar response, lobe and null structure and quarter-power angle as a function of frequency. The remaining sections represent largely new work and are summarized as follows:

First, the pressure response of a line source as a function of distance is shown to be dependent upon the path along which the response is calculated. Typically, a path is taken normal to the source beginning at its midpoint. This introduces symmetry into the model and produces a result that is unique to this origin and path. The paper illustrates how different responses are obtained by choosing alternate origins. The paper further notes that it is typical to use the midpoint of the source as the origin for the normal path to estimate transition distance. This understates the complexity of the transition from the near field to the far field. The paper suggests using pressure fields instead of pressure response to fully capture this complexity and derives the required mathematical expressions.

Second, “J” and progressive line sources are introduced and are shown to provide asymmetrical polar responses in the vertical plane. Such asymmetry is useful in many sound reinforcement venues and is why so many contemporary loudspeaker line arrays are based on these configurations. The paper provides analytical models for both types and illustrates typical performance. Of particular note, progressive arrays produce a vertical polar response that is remarkably constant with frequency over a very wide bandwidth.

Third, line arrays of real loudspeakers are not perfectly continuous line sources and this may introduce anomalies into their response. The paper provides a model that shows the effect of gaps in line sources that are introduced by the thickness of the loudspeaker enclosure construction material. The model shows that at low frequency, where the gap length is a small fraction of the wavelength, gaps have very little effect. At high frequency, the side lobe structure changes materially with gap length. The lobes get wider and change position. As a practical matter, contemporary loudspeaker line array enclosures are usually designed to maximize the radiating percentage, often in excess of 90%. This minimizes the effects of gaps across the useful bandwidth.

Fourth, real loudspeaker elements may not produce perfectly flat wave fronts so that a vertical stack of loudspeakers does not provide a perfectly straight-line source. The paper provides an analytical model to estimate the effect of curvature of the elemental sources of a line array. It shows that the effects are frequency dependent and negligible as long as the curvature is less than  $\frac{1}{4}$  wavelength.

Finally, measured polar response data of two different loudspeaker line arrays were compared to modeled results. Generally, the models produce very good estimates of actual performance despite the fact that loudspeaker non-linearities, enclosure diffraction and environmental effects among others are not accounted for. Robust results can be obtained for a wide variety of array types across an extended frequency range of interest.

## 10 ACKNOWLEDGEMENTS

The author would like to express his appreciation to his colleagues at JBL Professional including Mark Gander, David Scheirman, Mark Engebretson and Doug Button. They piqued his interest in line arrays, encouraged and supported this body of work and were always fun to work with.

## 11 REFERENCES

- [1] Klepper, David and Douglas Steele, “Constant Directional Characteristics from a Line Source Array”, Presented October 15, 1962 at the 14<sup>th</sup> annual fall convention of the Audio Engineering Society, New York.
- [2] Olson, Harry. F., Elements of Acoustical Engineering, 1st ed., p.25, D. Van Nostrand Company, Inc., New York, 1940.
- [3] Wolff, I., and Malter, L., “Directional Radiation of Sound”, Jour. Acous. Soc. Amer., Vol. 2, No. 2, p. 201, 1930. The seminal work on line arrays.
- [4] Beranek, Leo, Acoustics, first edition, McGraw-Hill, 1954. Author shows polar response (in dB) of line sources (p. 96) and curved sources (p. 106).
- [5] Wood, A. B., A Textbook of Sound, G. Bell and Sons, London, 1957.
- [6] Davis, A. H., Modern Acoustics, 1<sup>st</sup> ed., p. 63, The Macmillan Company, New York, 1934.
- [7] Rossi, M., Acoustics and Electroacoustics, Artech House, Norwood, MA., 1988.
- [8] Skudrzyk, E., The Foundations of Acoustics, Springer-Verlag, New York, 1971.
- [9] Lipshitz, Stanley and John Vanderkooy, “The Acoustic Radiation of Line Sources of Finite Length”, presented November, 1986 at the 81<sup>st</sup> annual convention of the Audio Engineering Society, Los Angeles, preprint 2417(D-4).
- [10] Smith, D. L., “Discrete-Element Line Arrays – Their Modeling and Optimization”, J. Audio Eng. Soc., Vol. 45, No. 11, 1997.
- [11] Heil, C., “Sound Fields Radiated by Multiple Sound Source Arrays”, presented at the 92nd Convention of the Audio Engineering Society, 1992 March, Vienna, preprint 3269. Author discusses the response of line arrays in the near field (Fresnel region) and the far field (Fraunhofer region).
- [12] Junger, M. and David Feit, Sound, Structures, and their Interactions, The MIT Press, 1972.
- [13] Ureda, Mark S., “Line Arrays: Theory and Applications,” Presented at the 110th Convention of the Audio Engineering Society, 2001 May, Amsterdam, preprint 5304. See page 6 for far field equation.

- 
- [14] Op. cit., Wolff, I., and Malter, L. See page 212 for a discussion on curved line sources.
- [15] Op. cit., Olson, Harry. F. See page 27 where Olson provides the directional characteristics of 60°, 90°, and 120° arc sources.
- [16] Rossi, M., Acoustics and Electroacoustics, Artech House, Norwood, MA., 1988. See page 134 regarding curvilinear arrays.
- [17] Ureda, Mark, “J and Spiral Line Arrays,” Presented at the 111<sup>th</sup> Convention of the Audio Engineering Society, 2001 December, New York, New York, preprint 5485.
- [18] IBID.
- [19] Urban, Marcel, C. Heil and P. Bauman, “Wavefront Sculpture Technology”, J. Audio Eng. Soc., Vol. 51, No. 10, 2003.
- [20] Button, Doug, “High Frequency Components for High Output Articulated Line Arrays”, presented at the 113<sup>th</sup> Convention of the Audio Engineering Society, Los Angeles, October 2002.
- [21] Engebretson Mark, “Directional Radiation Characteristics of Articulating Line Array Loudspeaker Systems”, presented at the 111<sup>th</sup> Convention of the Audio Engineering Society, New York, November 2001.
- [22] Benson, J. E., “Theory and Applications of Electrically Tapered Electro-Acoustic Arrays,” IREE International Electronics Convention Digest, pp. 587-589, August 1975. *Note that Benson solved for the – 3dB angle.*
- [23] Ureda, Mark, “Wave Field Synthesis with Horn Arrays,” Presented at the 100<sup>th</sup> Convention of the Audio Engineering Society, 1996 May, Copenhagen, Denmark, preprint #4144(B-3).

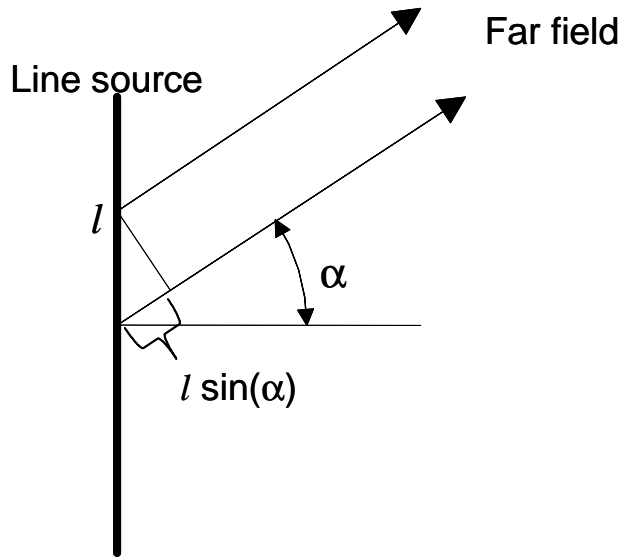


Figure 1: Geometric construction for the far field directivity function of a line source.

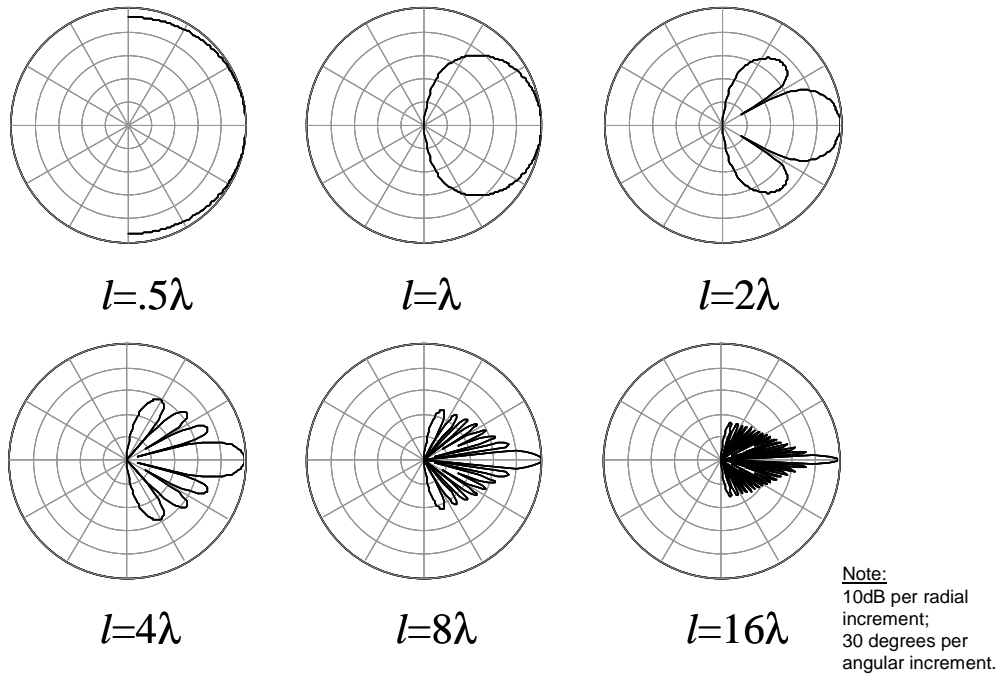


Figure 2: Polar response curves of a uniform line source.

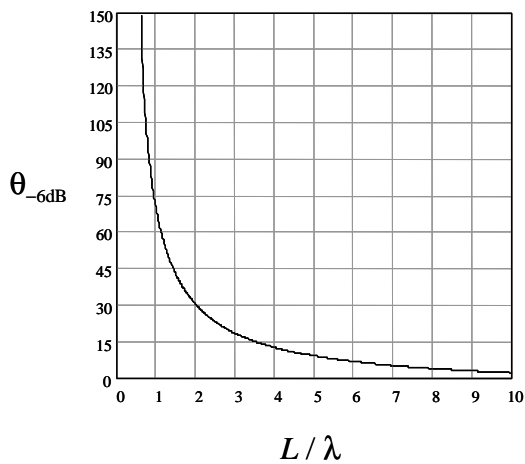


Figure 3: Quarter-power angle of a uniform line source.

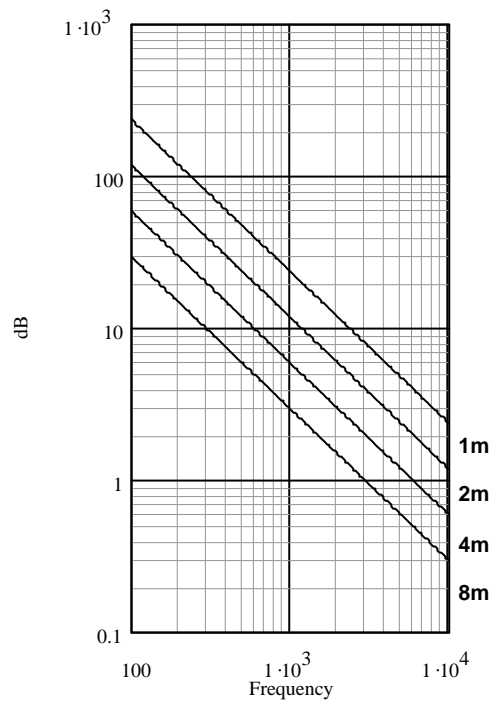


Figure 4: Directivity response of uniform line sources 1, 2, 4 and 8 meters long.

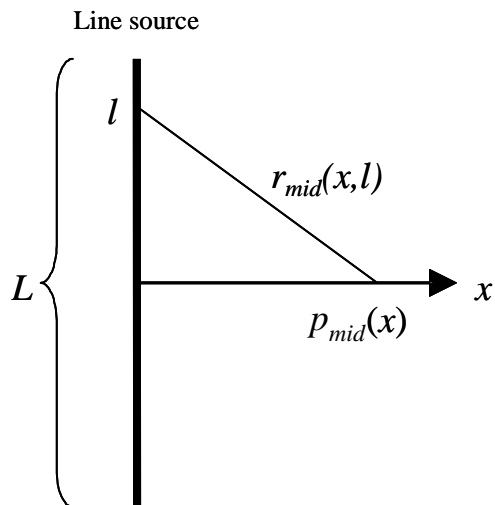


Figure 5: Geometric construction for calculating the on-axis pressure response of a line source (midpoint convention).

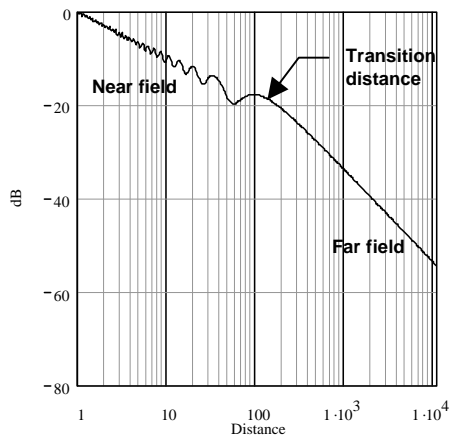


Figure 6: On-axis pressure response (from the midpoint) of a uniform line source (4m long, 8kHz).

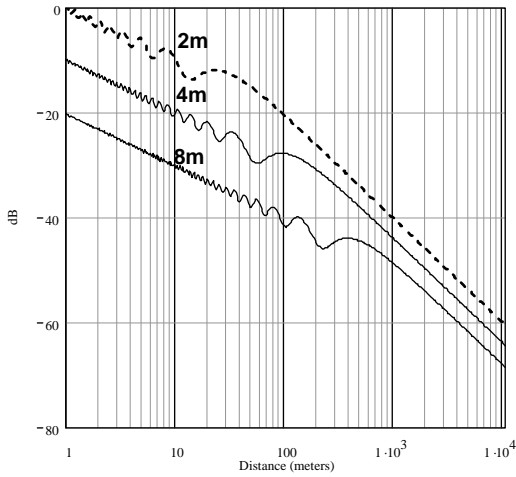


Figure 7: On-axis response (from the midpoint) of 2, 4 and 8 meter long uniform line sources at 8kHz. The 4 and 8 meter response curves are offset by 10dB and 20dB respectively.

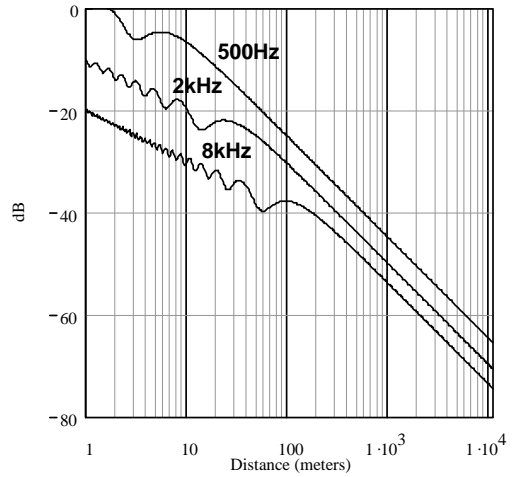


Figure 8: On-axis response (from the midpoint) of a 4-meter uniform line source at 500, 2kHz and 8kHz. The 2kHz and 8kHz response curves are offset by 10dB and 20dB respectively.

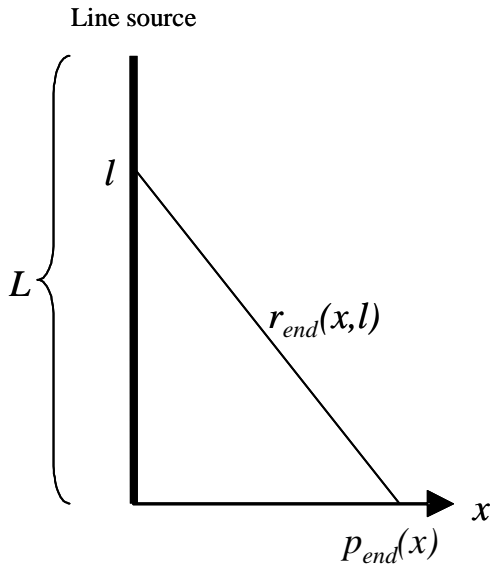


Figure 9: Geometric construction to calculate the pressure response along a path originating at the endpoint.

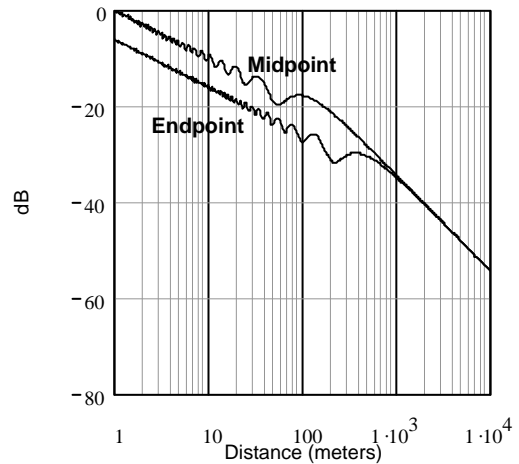


Figure 10: Comparison of midpoint and endpoint pressure response curves of a 4-m uniform line source at 8kHz.

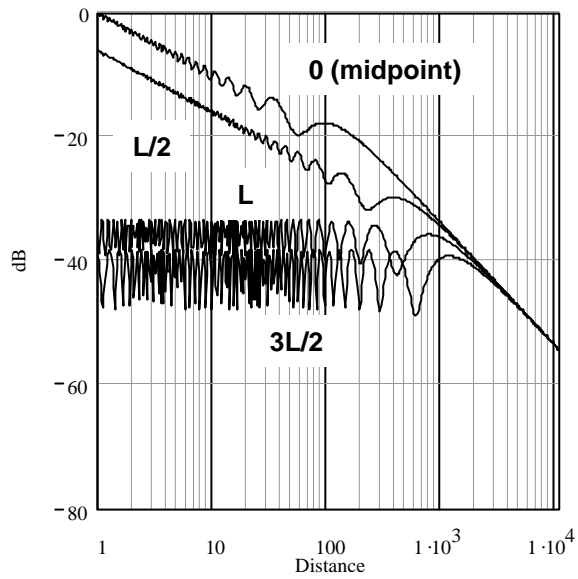


Figure 11: Pressure response along paths normal to the line source at various points of origin. (4-meter long at 8kHz)

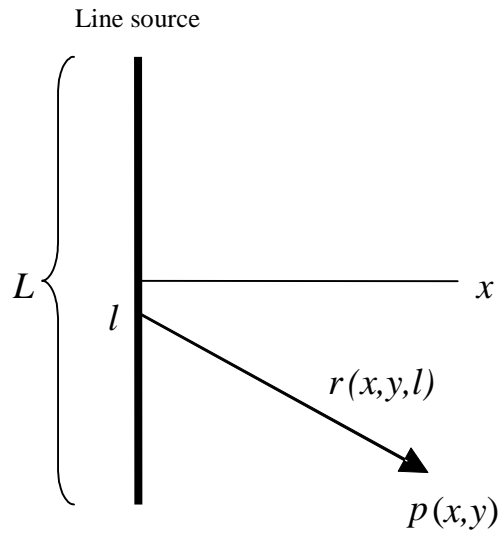


Figure 12: Geometric construction for pressure field of a line source.

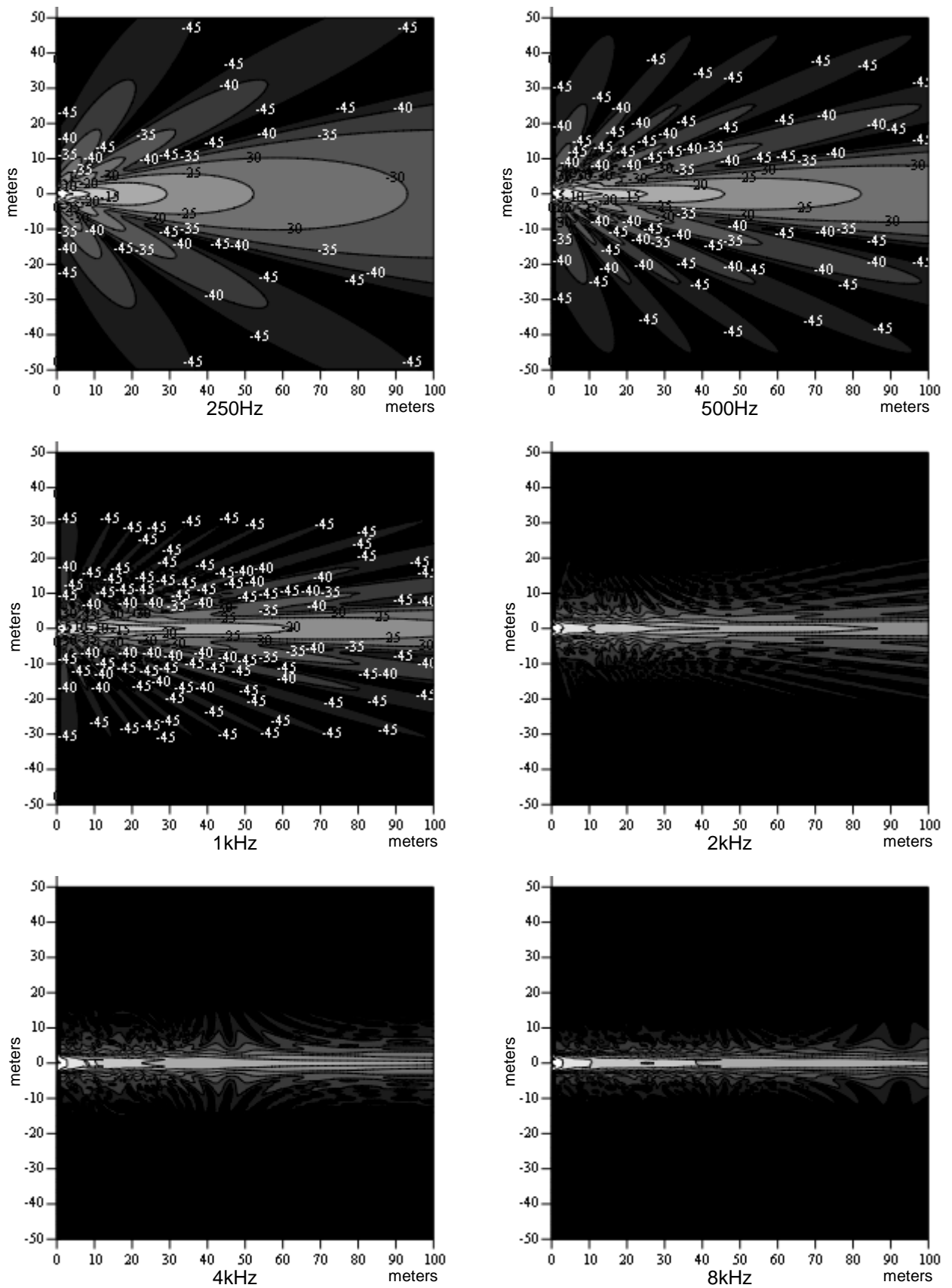


Figure 13: Pressure fields of a 4-m line source. The contour scale numbers are removed from the 2kHz, 4kHz and 8kHz plots for clarity.

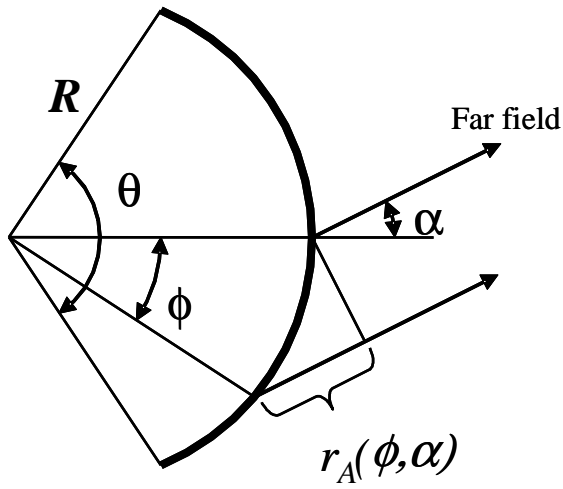
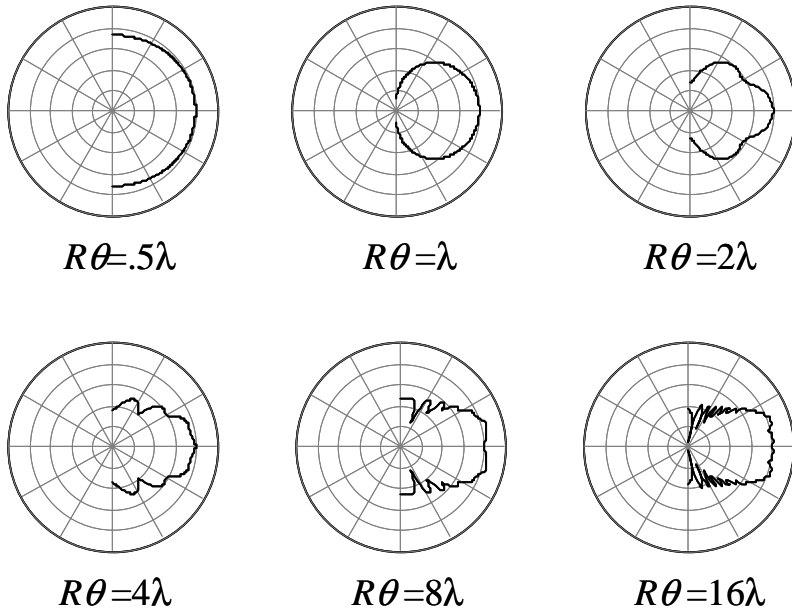


Figure 14: Geometric construction of an arc source for polar response.



Note:  
 10dB per radial  
 increment;  
 30 degrees per  
 angular increment.

Figure 15: Polar response curves of an arc source.

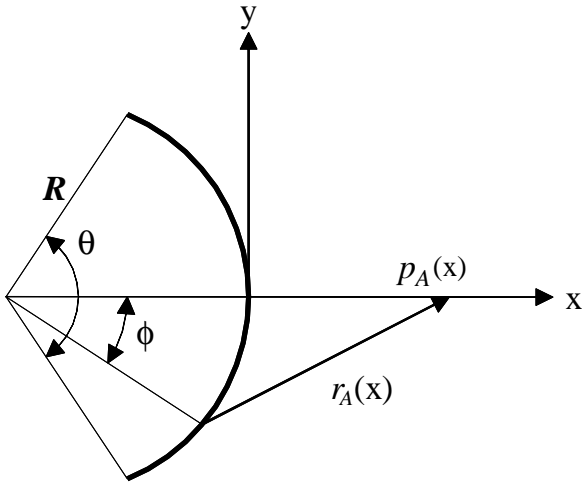


Figure 16: Geometric construction of an arc source for on-axis response.

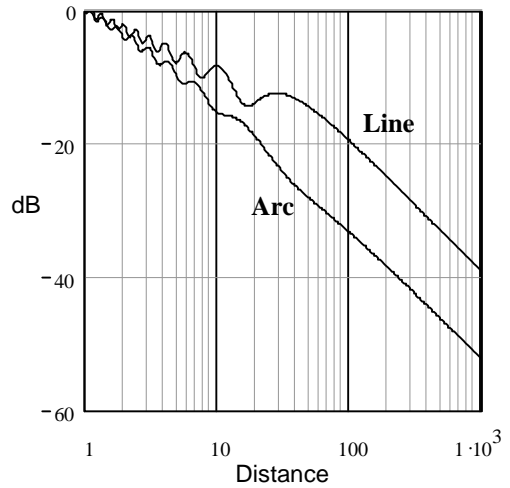


Figure 17: On-axis pressure response of an arc source and a straight line source at 4kHz. The arc source has an included angle of  $45^\circ$  and a radius of 4m. The line source has a length equal to the arc length (3.14m).

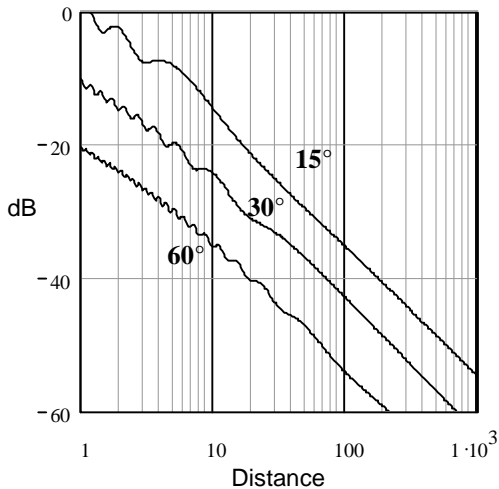


Figure 18: On-axis pressure response of three arc sources ( $\theta = 15^\circ, 30^\circ$  and  $60^\circ$ ) at 8kHz where  $R=4\text{m}$ . These correspond to arc lengths of approximately 1, 2, and 4 meters. The  $30^\circ$  and  $60^\circ$  curves are offset by 10 and 20 dB respectively.

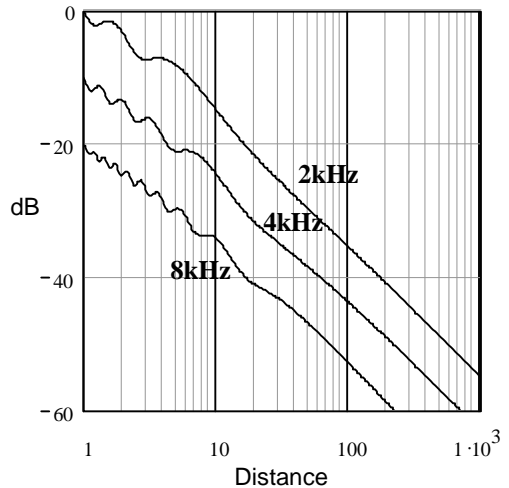


Figure 19: On-axis pressure response of an arc source at various frequencies where  $\theta = 30^\circ$  and  $R=4\text{m}$ . The arc length is approximately 2m. The 2kHz and 8kHz curves are offset by 10 and 20 dB respectively.

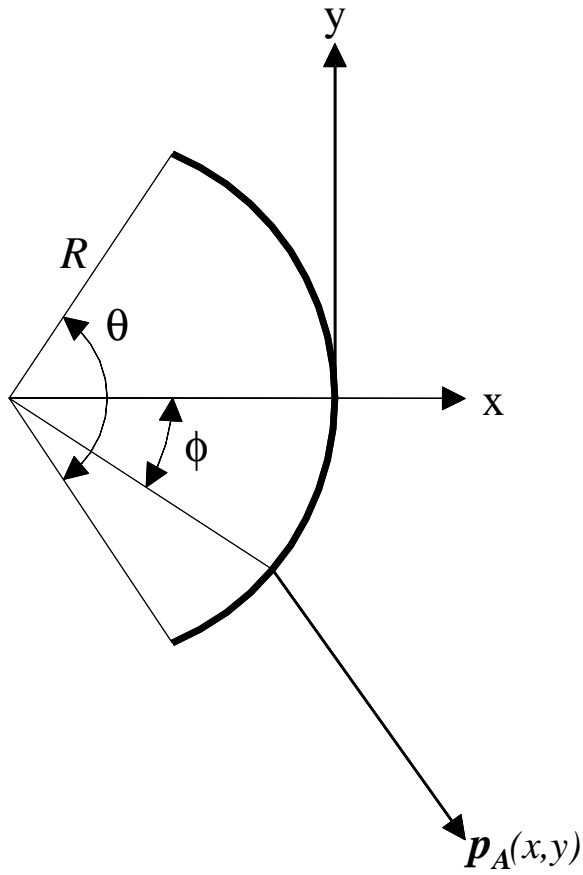


Figure 20: Geometric construction for arc source pressure field.

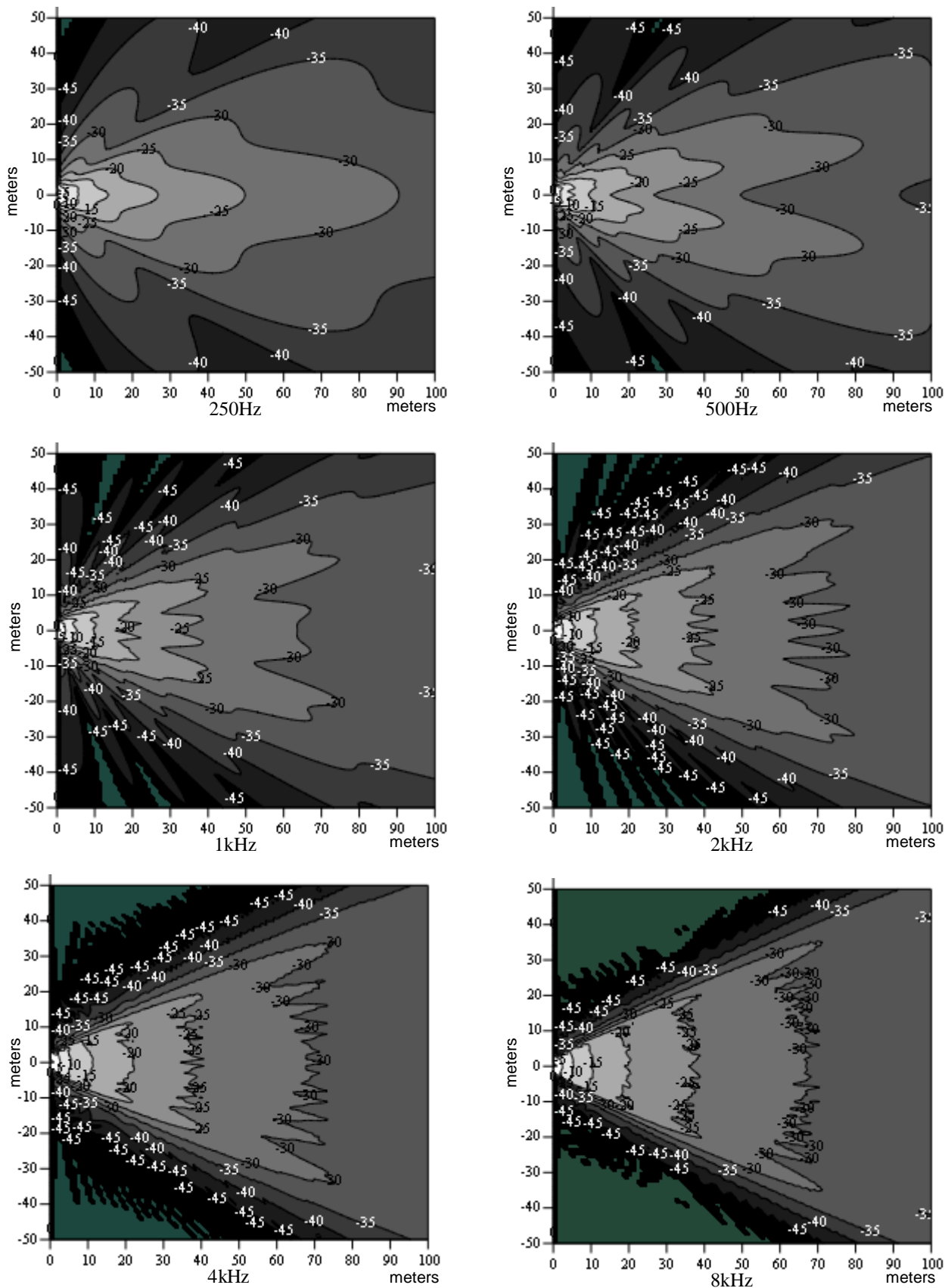


Figure 21: Pressure fields of a uniform arc source.

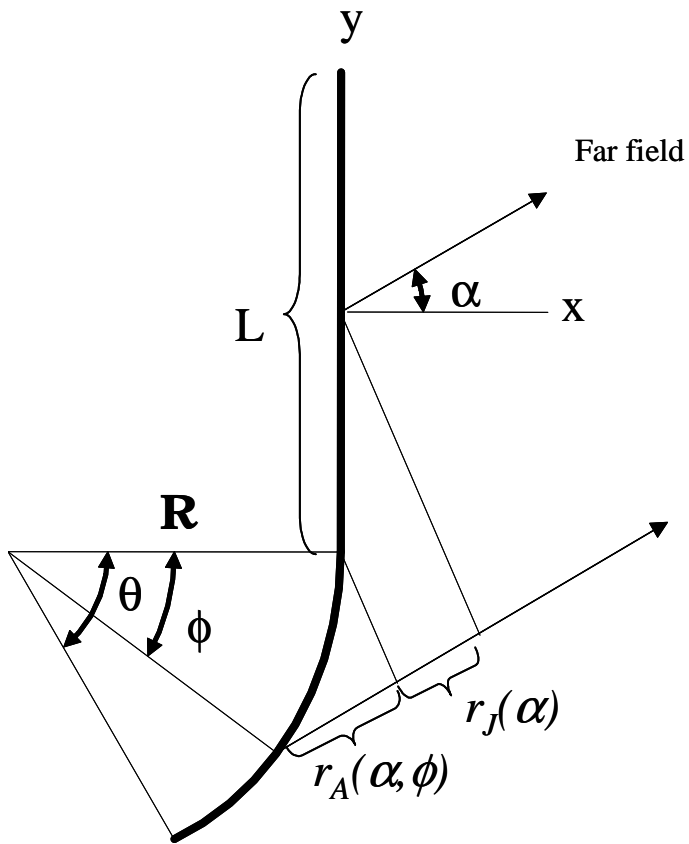


Figure 22: Geometric construction of a J-Source for polar response.

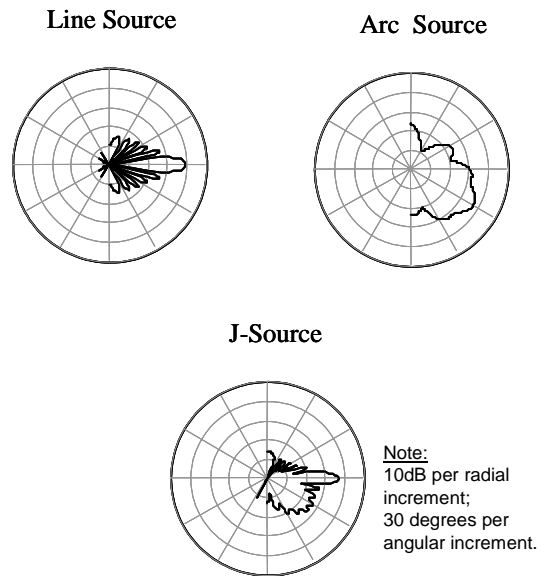
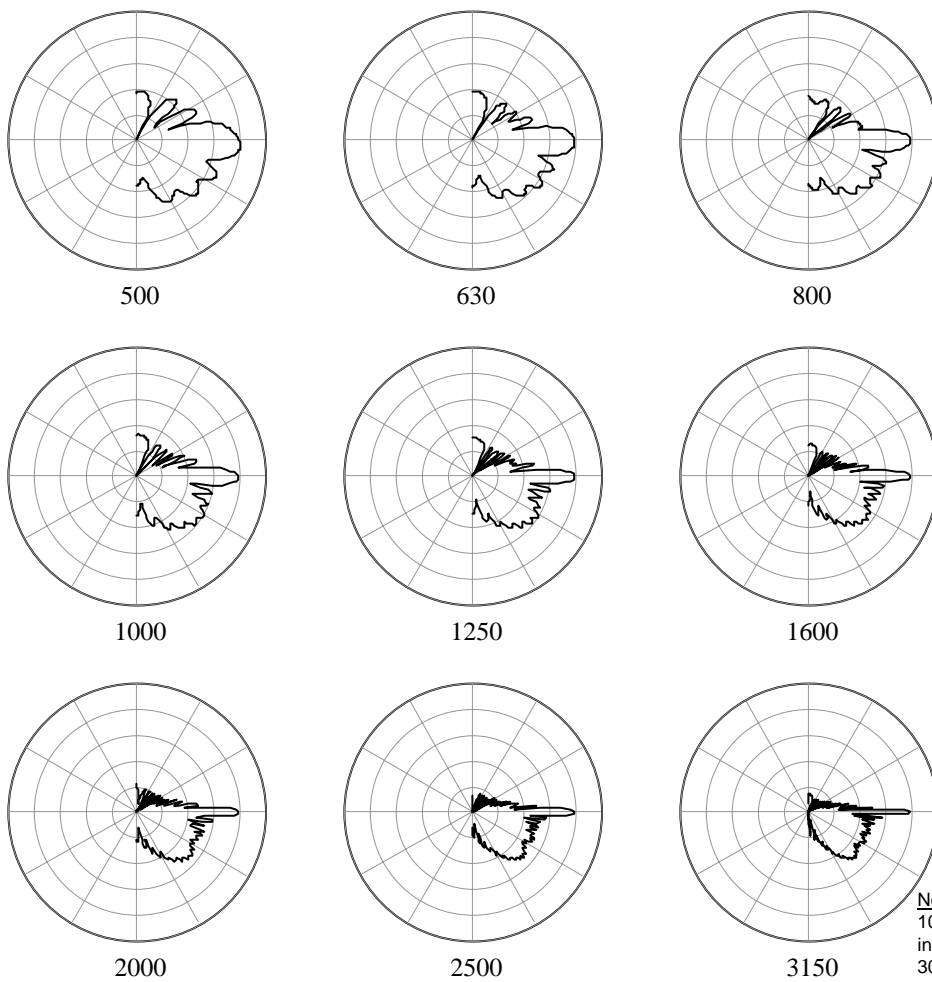
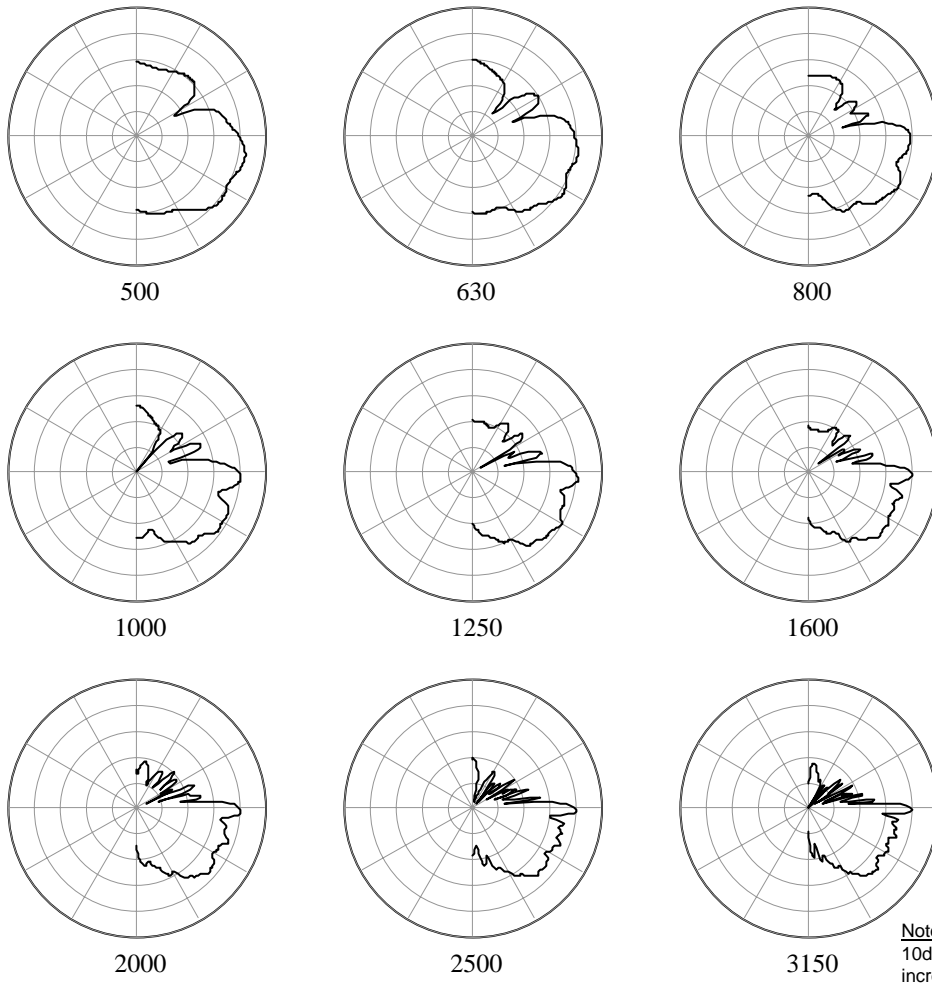


Figure 23: Contribution of a line and an arc source to the polar response of a J-Source



Note:  
 10dB per radial  
 increment;  
 30 degrees per  
 angular increment.

**Figure 24: J-source polar response curves – Example 1**  
 where  $L=2m$ ,  $R=1m$ ,  $\theta=60^\circ$ ,  $A_L=1$  and  $A_A = 1$ .



Note:  
 10dB per radial  
 increment;  
 30 degrees per  
 angular increment.

**Figure 25: J-source polar response curves – Example 2**  
 where  $L=1m$ ,  $R=1m$ ,  $\theta=60^\circ$ ,  $A_L=1$  and  $A_A = 2$ .

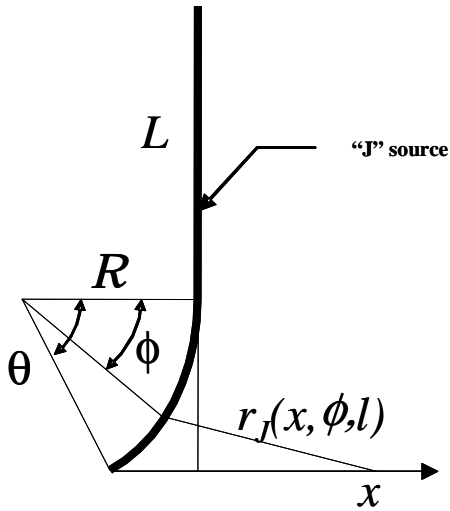


Figure 26: Geometric construction of a J-source for on-axis pressure response.

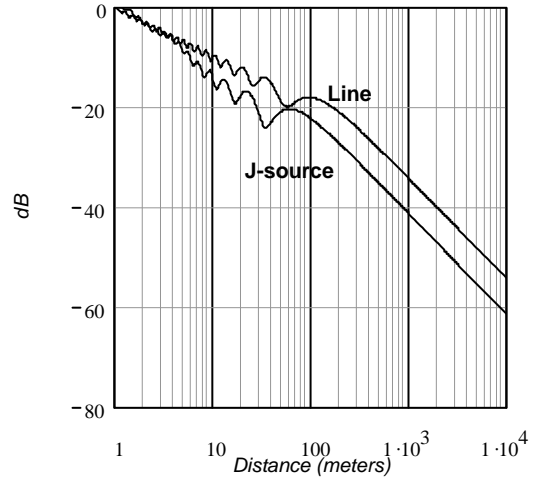


Figure 27: Comparison at 2kHz of the on-axis pressure response of a 4 meter long straight line source and a J-source where  $L=2m$ ,  $R=2m$ ,  $\theta=60^\circ$ ,  $A_L=1$  and  $A_A = 1$ .

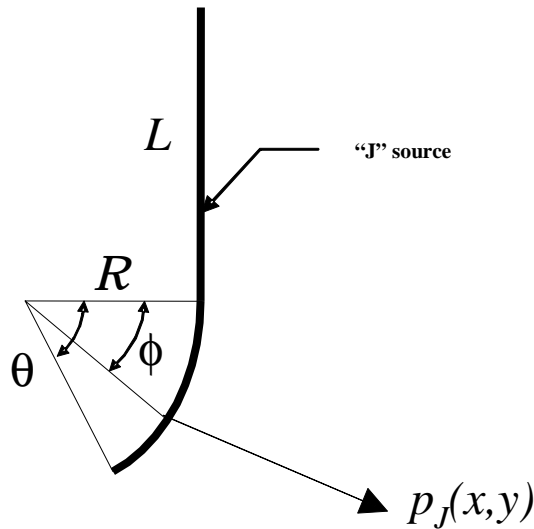


Figure 28: Geometric construction for the pressure field of a J-source

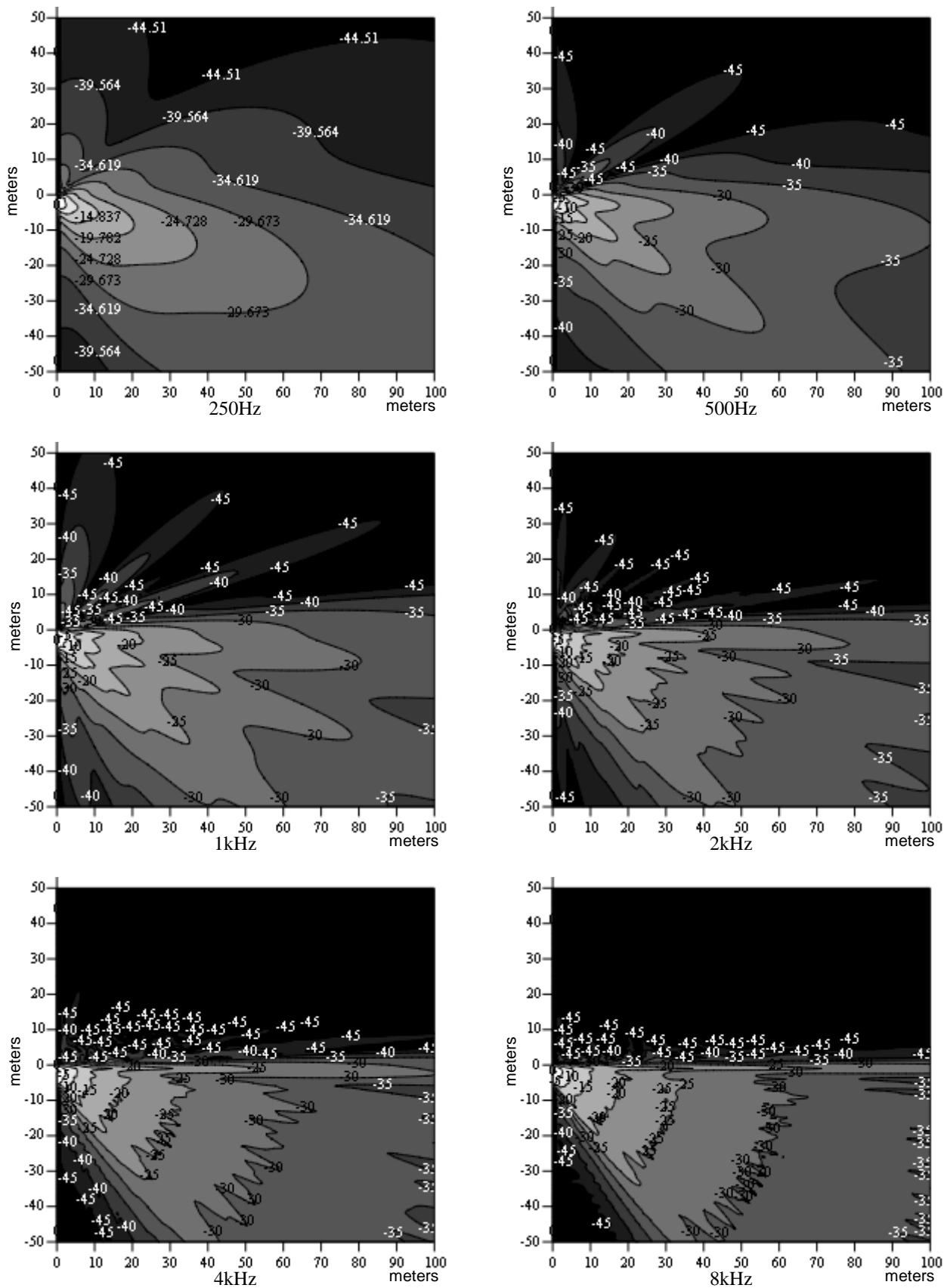
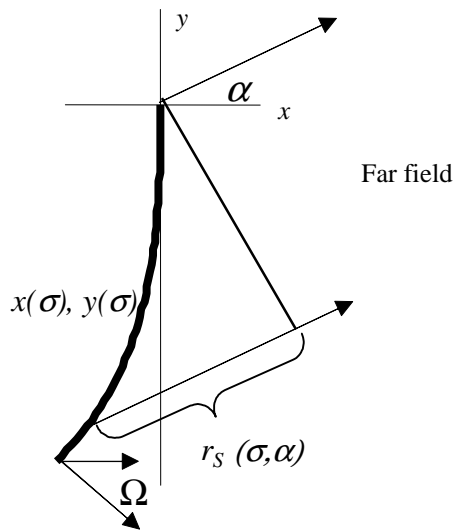
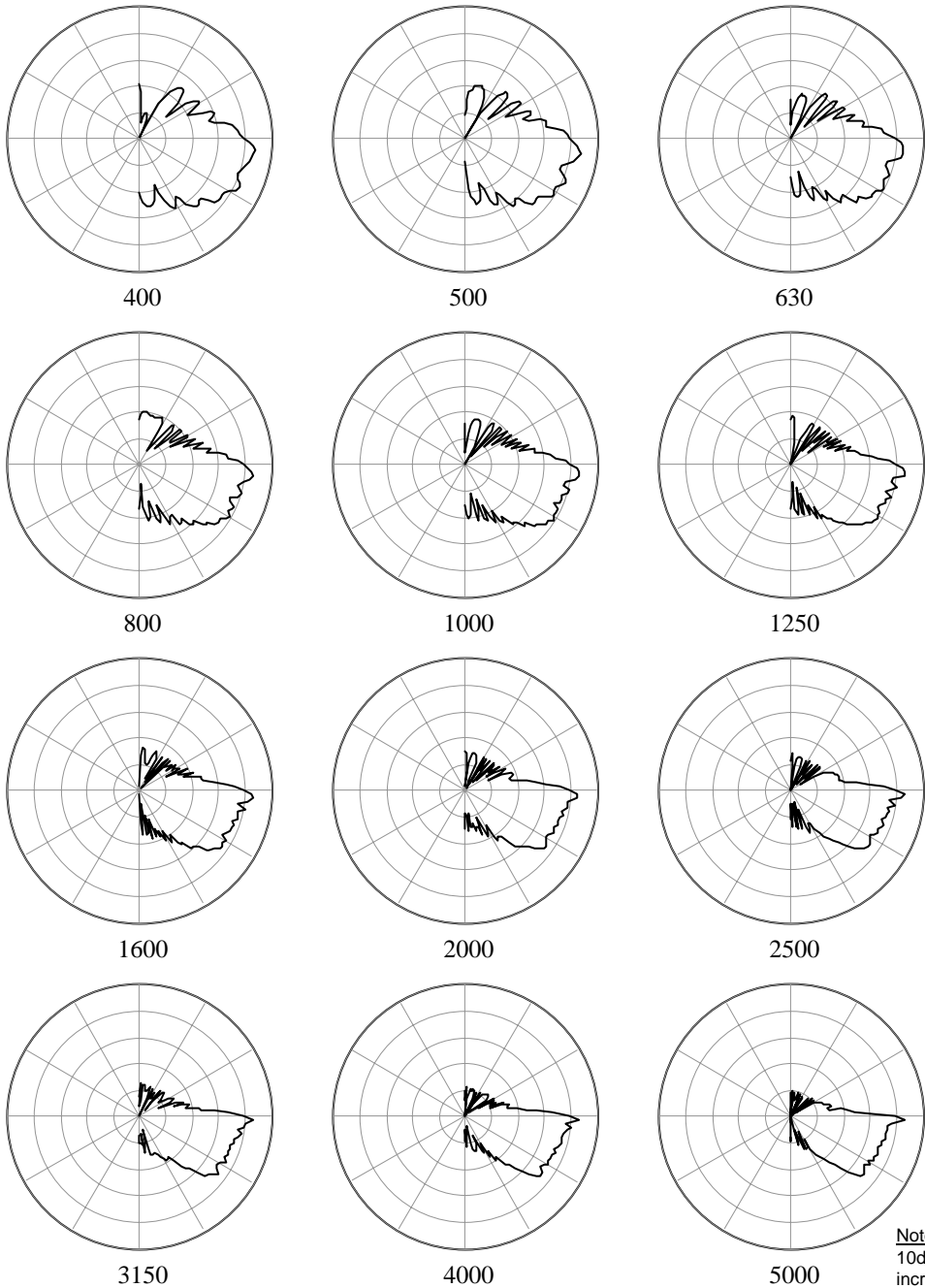


Figure 29: Pressure field of a J-source vs. frequency



**Figure 30: Geometric construction of a spiral source for polar response.**



Note:  
 10dB per radial  
 increment;  
 30 degrees per  
 angular increment.

**Figure 31: Polar response of a 5 meter long spiral source with a terminal angle of 45°.**

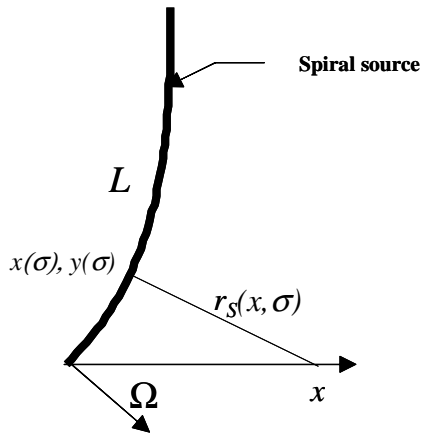


Figure 32: Geometric construction of a spiral source for on-axis pressure response.

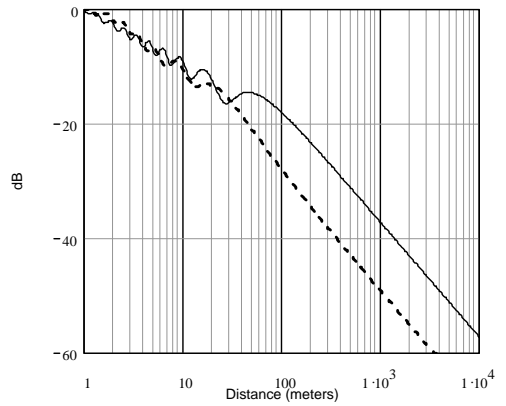


Figure 33: Pressure response comparison at 2kHz of a 45° terminal angle, 4 meter long spiral source and a line source of the same length.

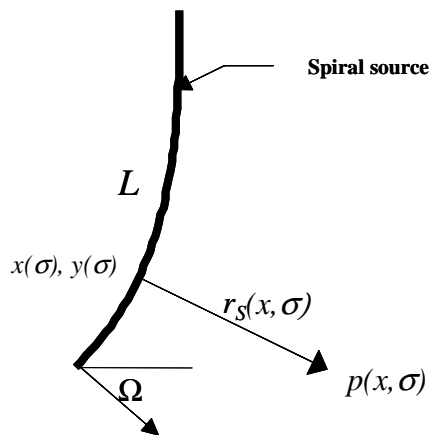


Figure 34: Geometric construction for pressure field of spiral source.

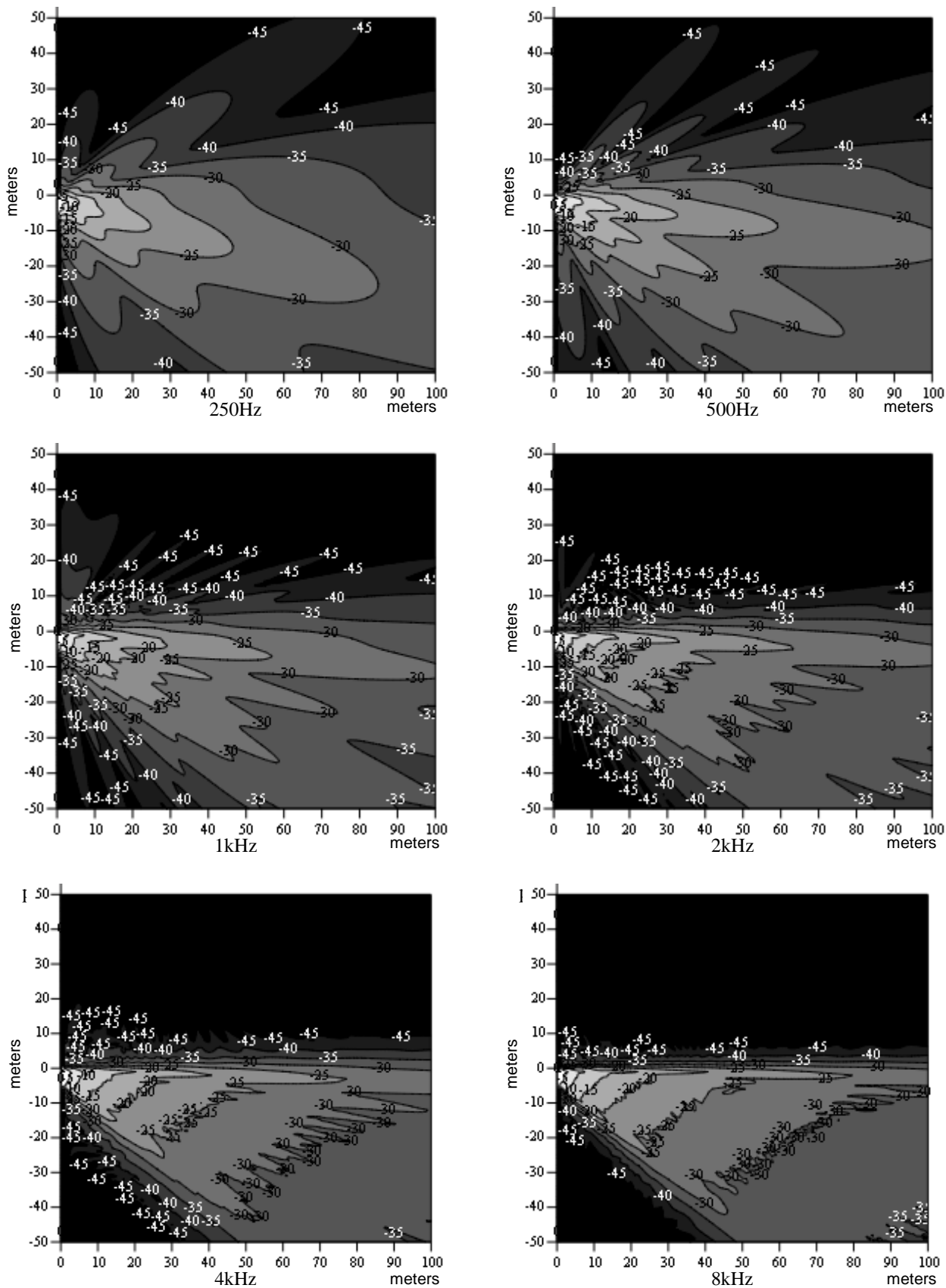


Figure 35: Pressure fields of spiral source vs. frequency.

Stack of four  
line sources  
with gaps.



The radiating  
ratio of a  
single source  
is  $(L-2d)/L$ .

**Figure 36: Line array of four elements of length  $L$  and non-radiating gap  $d$  on either end.**

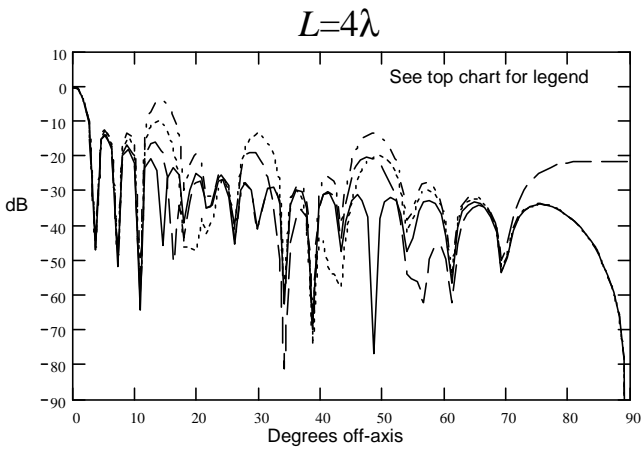
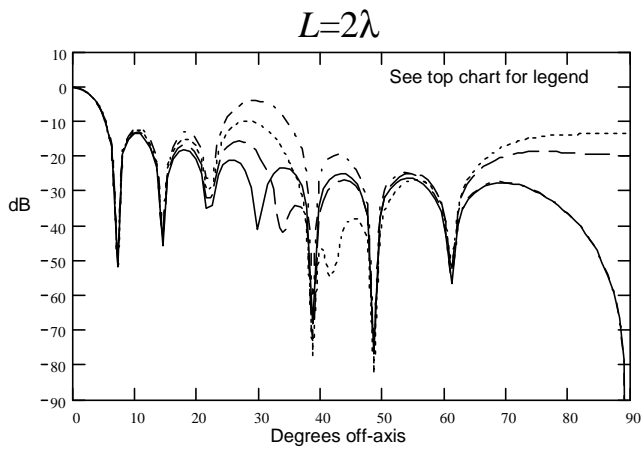
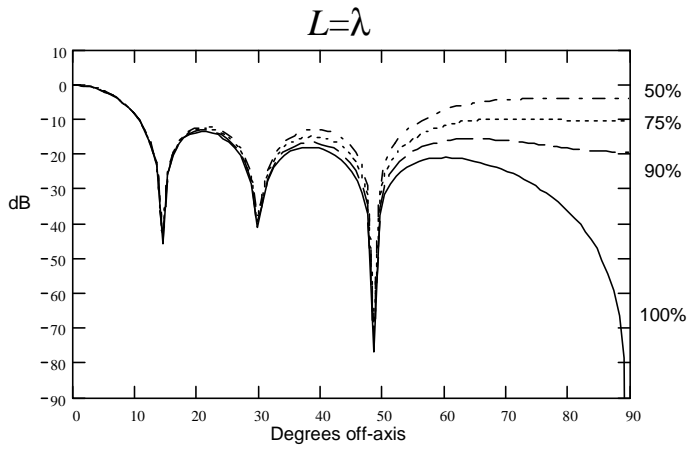


**Figure 37: Directivity function of a 4-element line array with radiating percentages of 100%, 90%, 75% and 50% at three ratios of length to wavelength.**

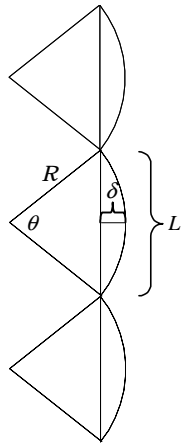


**Figure 38: Stack of three arc sources of radius  $R$ , included angle  $\theta$  and curvature  $\delta$**

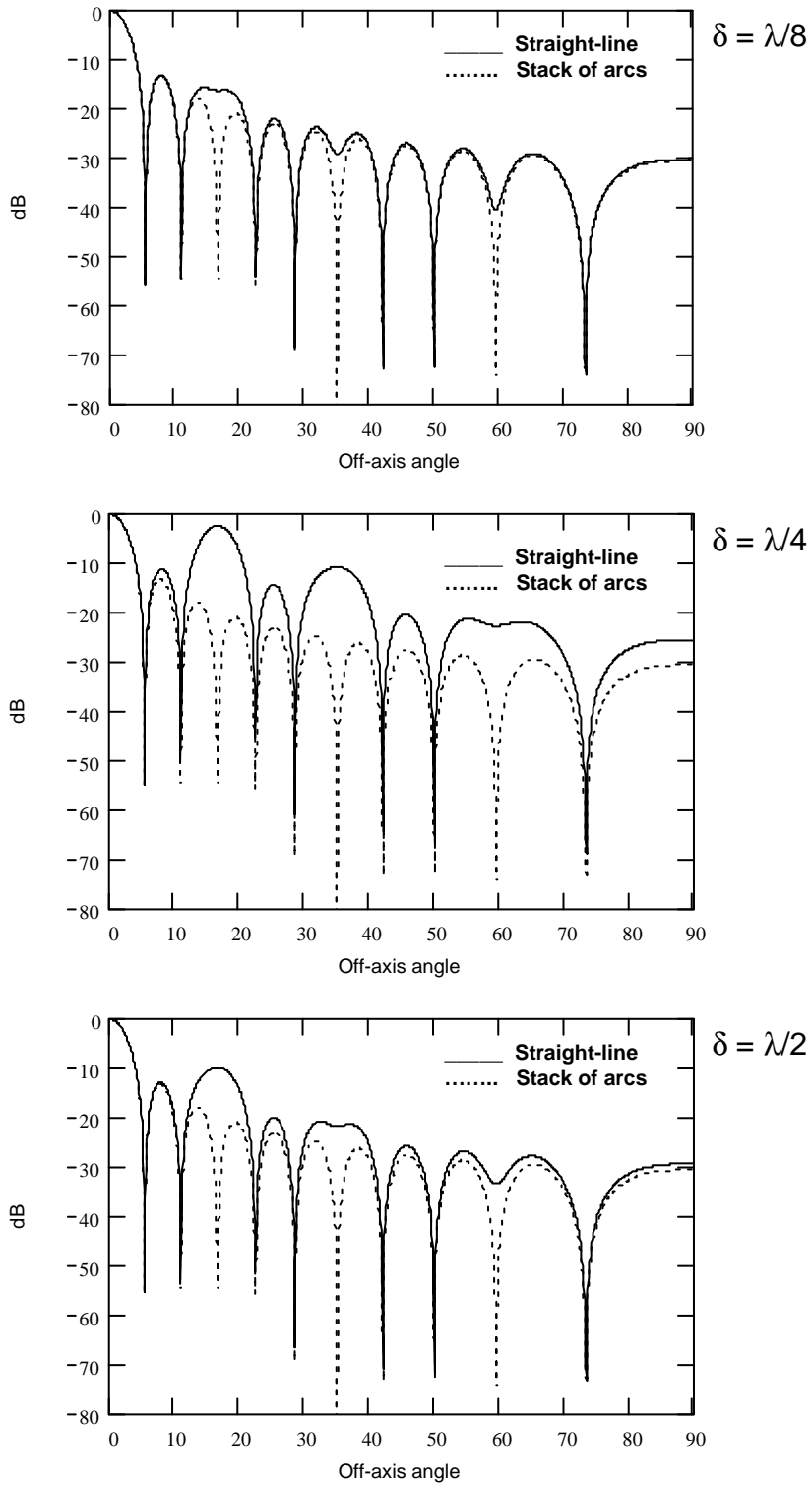


**Figure 39: Comparison of directivity functions of a stack of three curved sources (solid line) and a straight-line source (dotted line). The curved sources have an element length  $L$  of 15cm and a total included angle  $\theta$  of 20 degrees. The straight-line source has a total length of  $3L$ .**

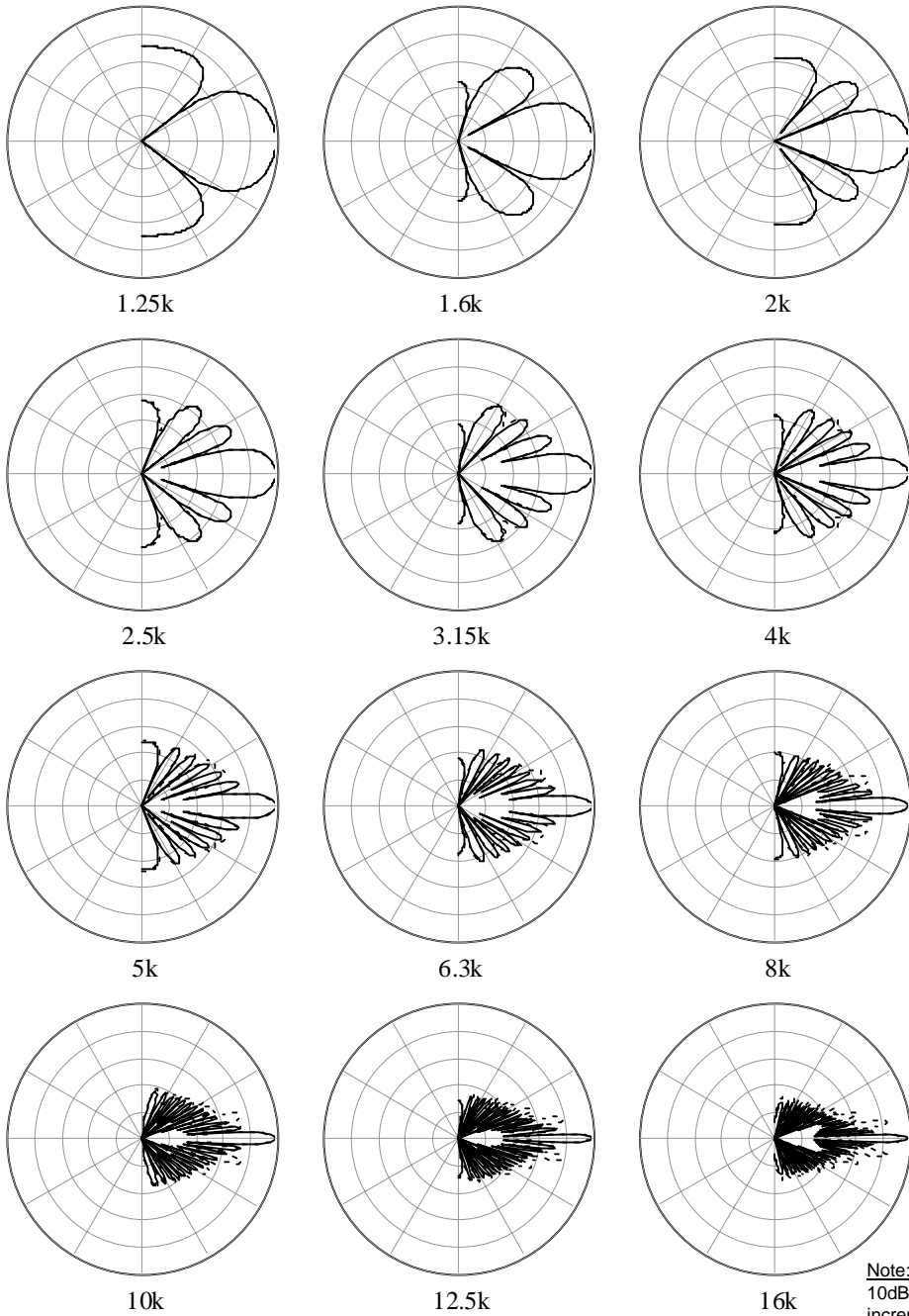


**Figure 40: Polar response curves of a stack of three 15cm high, 20° arc sources (dotted line) superimposed over the response of a 45cm straight line source (solid line).**

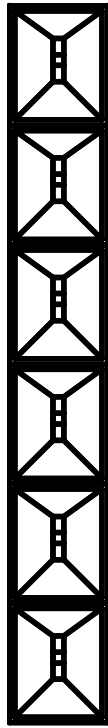


Figure 41: Vertical stack of six 8 inch tall, 40° x 20° degree horns.

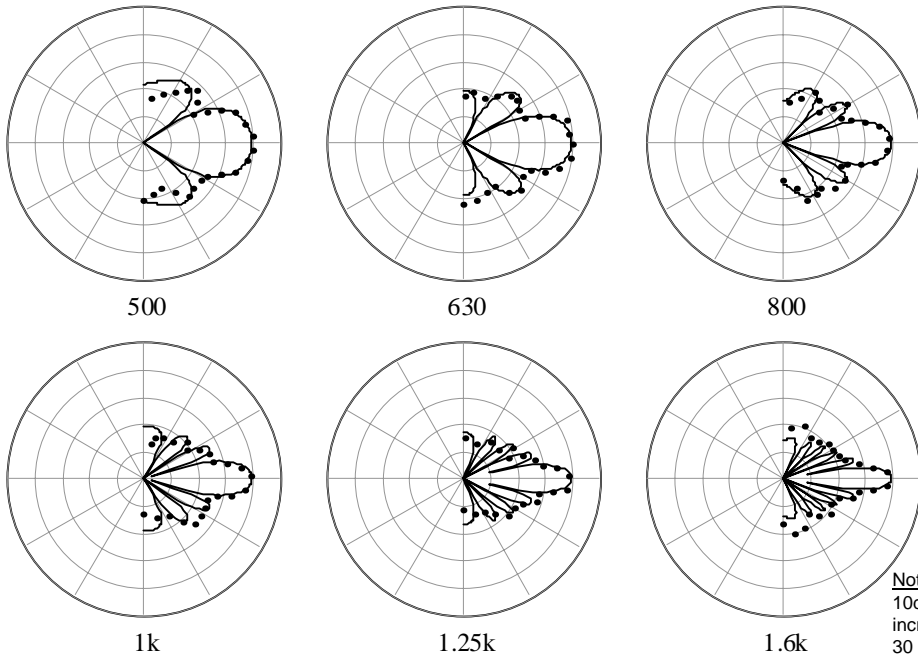
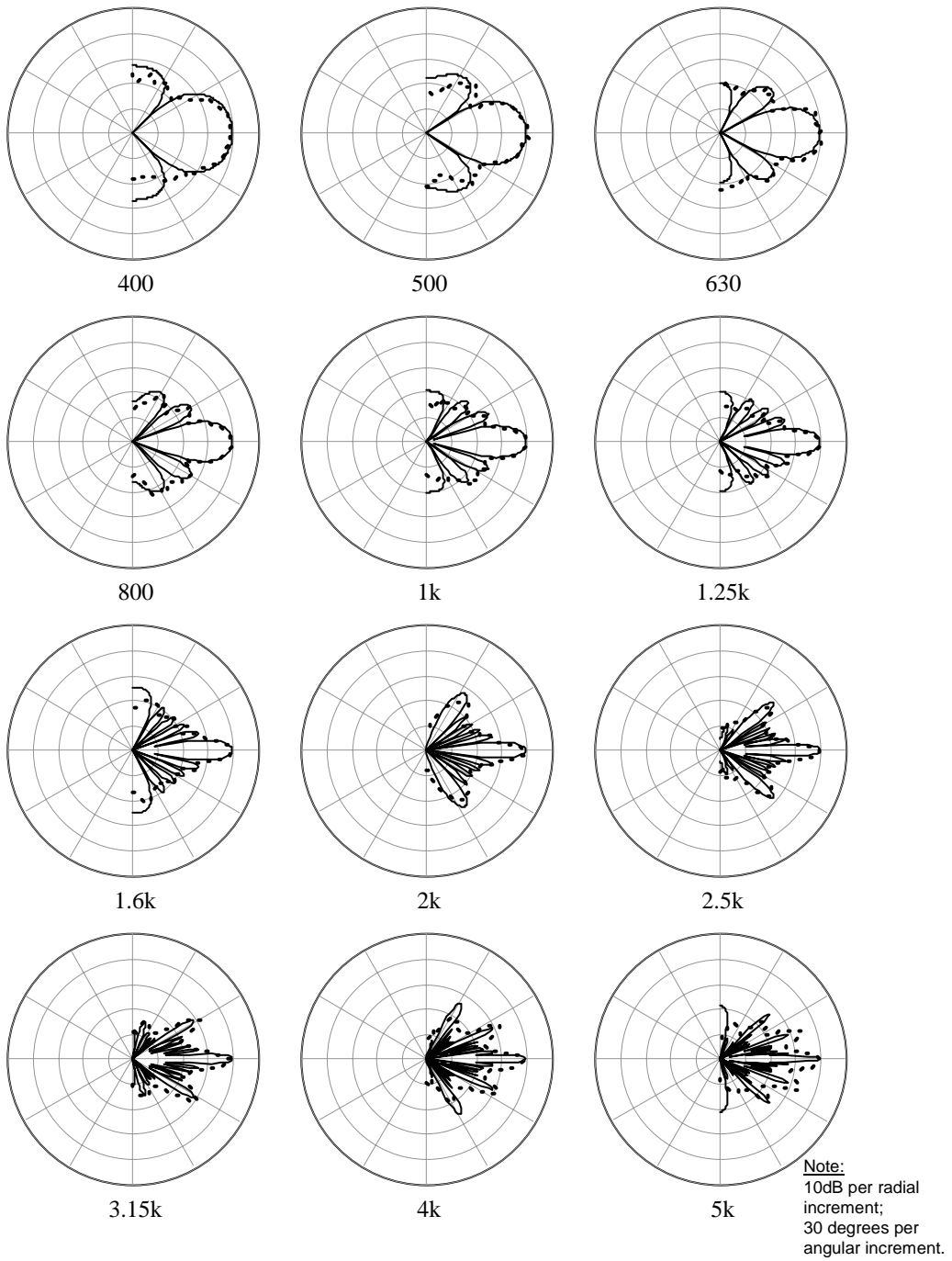


Figure 42: Measured (dots) versus modeled (solid line) polar response curves of the array in Figure 41. Model based on uniform straight line source and a sine wave input. Measured data is 1/3 octave pink noise.



**Figure 43: Measured (dots) versus modeled (solid line) polar response curves of the array in Figure 41. Model based on a stack of arc sources with a sine wave input. Measured data is 1/3 octave pink noise.**



**Figure 44: Indoor ground plane setup for vertical polar response measurement of an eight element curved array.**

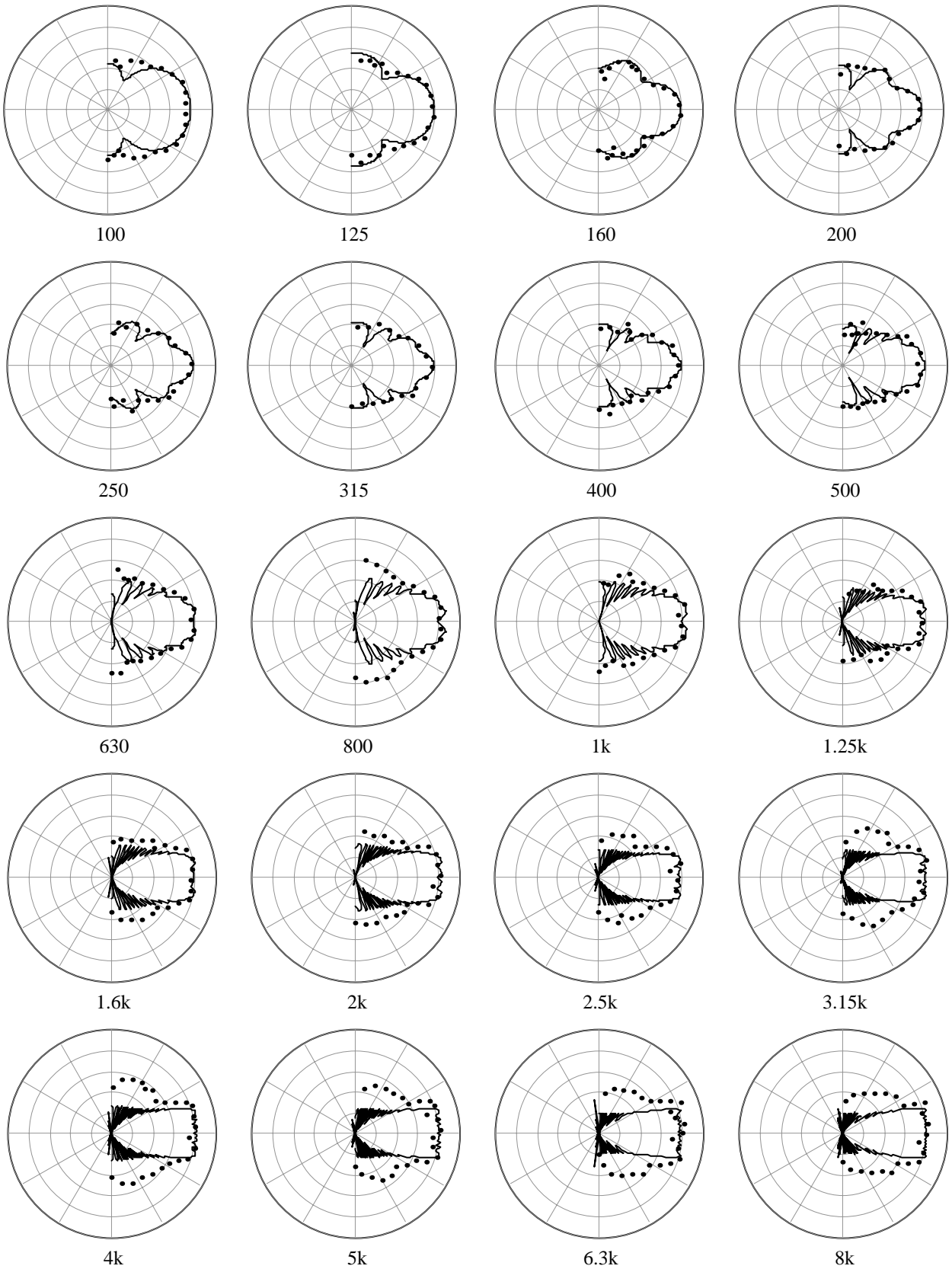


**Figure 45: Measured polar response data (dots) shown against predicted polar response of eight element curved array.**

Note:  
 10dB per radial  
 increment;  
 30 degrees per  
 angular increment.